Macroeconomic and Financial Risks:
A Tale of Mean and Volatility[*]

Dario Caldara[†]   Chiara Scotti[‡]   Molin Zhong[§]

April 21, 2023

Abstract

This paper investigates the drivers of uncertainty and tail risk of future GDP growth and corporate credit spreads using a stochastic volatility vector autoregression. We identify shocks using sign and zero restrictions on the model coefficients. We find that adverse macroeconomic and financial shocks lead to an increase in uncertainty and downside tail risk concerning future GDP growth and corporate spreads, but only to a small reduction in upside tail risk. Macroeconomic shocks have a significant impact on uncertainty and downside risk at shorter horizons, while financial shocks account for most of the variation at longer horizons.

KEYWORDS: Uncertainty; Tail Risk; Stochastic Volatility; Structural Identification.
JEL CLASSIFICATION: C32. E44.

1 Introduction

Uncertainty about future economic outcomes is crucial for economic decisions and for policy-making. A vast empirical and theoretical literature discusses how households and firms respond to high levels of economic uncertainty and downside risk, the latter defined as the risk of particularly large adverse events materializing.[1] A highly uncertain and risky economic outlook can cause concerns among policymakers and influence policy decisions. For instance, a study by Evans et al. (2015) found evidence of risk management considerations—the assessment of what could go wrong with the economy and judging whether policy should be adjusted to minimize risks—in one-third of the Federal Open Market Committee monetary policy decisions between 1993 and 2008. Managing risks originating in the financial sector is a key goal of macroprudential policy.

This paper investigates the drivers of uncertainty and tail risk of future economic conditions, measured by GDP growth, and future financial conditions, measured by corporate credit spreads, using a stochastic volatility vector autoregression (SV-VAR). In the model, the mean of the endogenous variables influence their unobserved volatility and, similarly, volatility feeds back into the mean.

We distinguish between shocks originating in the real economy and shocks originating in the financial sector. Accordingly, we propose an identification scheme that identifies macroeconomic and financial shocks imposing sign and zero restrictions on the contemporaneous structural coefficients of the model. We discipline the simultaneous feedback between GDP growth, GDP growth volatility, and corporate spreads imposing sign restrictions in line with results of workhorse DSGE models, in which financial conditions can impact economic activity and vice versa (for instance Bernanke et al. 1999). We use zero restrictions to impose that there is one financial shock driving the high correlation between credit spreads and its volatility observed in the data. The appeal of our approach is that it does not restrict the sign or size of the impulse responses to the structural shocks, and all shocks can potentially generate sizeable movements in macro and financial indicators. In addition, the restrictions we impose are compatible with a set of structural models rather than a unique one (Rubio-Ramirez et al., 2010; Arias et al., 2018).

Figure 1 illustrates our main findings plotting the distributions for 1-year-ahead GDP growth and

---

[1]See for instance Bernanke (1983); Christiano et al. (2014); Gilchrist et al. (2014); Fernández-Villaverde et al. (2015); Jurado et al. (2015); Basu and Bundick (2017).

Figure 1: THE IMPACT OF MACRO AND FINANCIAL SHOCKS ON CONDITIONAL DISTRIBUTIONS
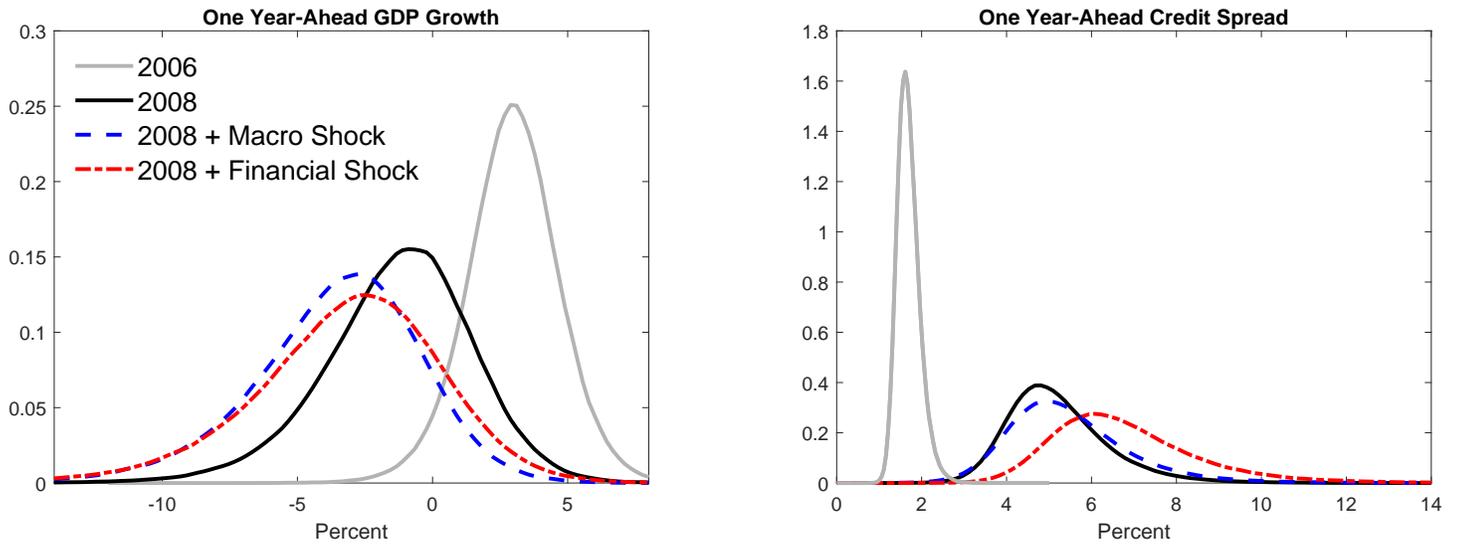
NOTE: The figure plots one year-ahead conditional distributions of average GDP growth and corporate credit spreads generated by our stochastic volatility VAR model. The gray distributions are computed conditioning on 2006:Q4 data, corresponding to a quarter of low volatility; the black distributions are computed conditioning on 2008:Q4 data, a quarter of high volatility. The blue (red) distributions are computed by running a counterfactual that adds to the baseline forecast in 2008:Q4 a two-standard deviation macro (financial) shock in 2009:Q1.

corporate credit spreads conditioning on data available at the end of 2008. The black solid lines show the baseline forecast, while the blue dashed and red dotted lines depict two counterfactual forecasts which assume that at the beginning of 2009 the economy is hit by a two-standard deviation macroeconomic and financial shock, respectively. We define uncertainty as the standard deviation of the conditional distributions of future GDP growth and credit spreads, and tail risk as the size and location of the tails of these distributions.

We emphasize two results. First, we find that adverse macroeconomic and financial shocks move simultaneously future GDP growth and corporate spreads. Second, these shocks generate an increase in uncertainty and downside tail risk of future GDP growth and spreads, but only a small reduction in upside tail risk. This is visible by noticing that the counterfactual distributions are more dispersed than the baseline distributions and place higher probability around particularly bad outcomes relative to good outcomes. The differential response of downside and upside risk happens because in our model shocks that lower the mean forecast also raise uncertainty around the forecast, thus increasing the probability of adverse tail outcomes relative to positive outcomes.

2

We also find that the effects of the shocks are stronger in periods of high volatility, such as in 2008, relative to periods of low volatility. As shown in Figure 1, low volatility periods such as 2006 feature substantially lower uncertainty and risk about future outcomes than periods of high volatility. Additionally, the relative importance of shocks varies across horizons. The effect of macroeconomic shocks is largest within the first year, while financial shocks play a dominant role at longer horizons (not shown in the figure).

We estimate the model using Bayesian techniques and compute conditional distributions as in Del Negro and Schorfheide (2013). These distributions reflect uncertainty about the realization of future shocks, the parameters of the model, and the underlying volatility states. We trace the nonlinear effects of shocks by constructing impulse responses of uncertainty and tail risk from the conditional densities. These effects materialize through three channels. First, a volatility channel, as shocks alter the evolution of current and future volatility. Second, an estimation-uncertainty channel, as parameter and state uncertainty make the effects of shocks more uncertain, particularly around downturns. Finally, a "higher-order" channel operating through the interaction between structural shocks and time-varying volatility beyond the direct effect of shocks on current and future volatility. Throughout the paper, we distinguish uncertainty from volatility, defining the latter as the standard deviation of the reduced-form innovations.

The result that macro and financial shocks generate uncertainty and downside risk is consistent with theories of macro and financial factors acting both as independent drivers of fluctuations or as amplifiers of adverse shocks. For instance, adverse demand shocks or financial panics can increase the probability that future negative shocks are amplified because of financial constraints, such as in models with borrowing constraints (Bocola, 2016)—or because of policy constraints, such as the effective lower bound on policy rates. Our results also have direct implications for risk management policies, as we distinguish between risks driven by macro and financial shocks. For instance, risks related to macro fundamentals can be addressed by changing the stance of monetary and fiscal policy, while risks originating in the financial industry can be more directly tackled with macroprudential tools.

The contribution of our paper can be best assessed in relation to three highly influential streams of literature. First, a growing number of papers have measured and forecasted downside risk to GDP

growth, also known as growth-at-risk. In their seminal work, Adrian et al. (2019) found that growth-at-risk can be forecasted primarily by financial data capturing deteriorating financial conditions. This finding has been questioned by Plagborg-Møller et al. (2020), which concludes that "financial variables contribute little to such distributional forecasts [of GDP growth], beyond the information contained in real indicators." Our use of a structural model reveals that macro and financial shocks move simultaneously macro and financial variables and are both drivers of uncertainty and tail risk.

Second, our model generates variation in uncertainty and tail risk exploiting the correlation between mean and volatility dynamics, an empirical regularity that finds strong support in the literature. This correlation is at the center of a growing number of papers employing SV-VARs to estimate the effects of shocks to time-varying volatility on the mean of the variables. We add to most of this literature by employing a novel identification strategy to identify macro and financial shocks—as studies mainly rely on recursive identification. We also go beyond the mean effects of shocks, documenting that these models have broad appeal for the joint measurement of uncertainty and risk and the study of their sources of variation. Our work uses the econometric specification of Mumtaz (2018), and relates to Carriero et al. (2023), who discuss the performance of SV-VAR for measuring risk, comparing the density and quantile forecasting properties of the model to quantile regressions.[2]

Finally, our analysis is also closely related to the literature using linear VARs to examine the relationship between uncertainty and the business cycle, such as Bloom (2009) and Ludvigson et al. (2021).[3] We offer insights that cannot be directly derived from linear VARs. In a linear model, shocks can only have mean effects, that is, they can only shift the location of the distributions plotted in Figure 1. Instead, we show how shocks shape the conditional distribution of future economic conditions beyond the mean, focusing on uncertainty and tail risk, and how the effects of shocks are nonlinear and vary with the overall level of volatility.[4]

---

[2]The literature on SV-VAR built on the work of Primiceri (2005) and Cogley and Sargent (2005). Insightful papers using SV-VAR models include, among many, Mumtaz and Zanetti (2013), Creal and Wu (2017), Carriero et al. (2018), and Shin and Zhong (2020).

[3]This literature includes studies that construct proxies of uncertainty and risk using textual analysis (Baker et al., 2016) or economic data releases (Scotti, 2016), and trace their economic effects using linear VARs. Cascaldi-Garcia et al. (2023) review this literature.

[4]Ludvigson et al. (2021) identify shocks using event and external variable constraints so that shocks have defensible properties during specific historical episodes. The level effects of our shocks are broadly in line with those of the macro shock and uncertainty shocks identified in their paper, even though our identification is based on sign and zero restrictions.

The use of only one macroeconomic and one financial indicator might seem an extreme assumption, but it is a natural one to make. The debate in the literature is about macro versus financial determinants of the conditional distribution of GDP growth. Prior work uses relatively small models, typically estimated on data for GDP growth, a financial factor, and occasionally a real activity factor. These factors summarize information from large panel datasets. Our parsimonious approach avoids complexities introduced by larger models and by the details of the factor extraction, allowing us to focus on the intrinsic logic of shock identification and on model mechanisms that are of broad applicability.[5]

The paper is organized as follows. Section 2 presents our modelling framework. Section 3 presents the estimates of the unobserved volatility states and of the model parameters. We find that the volatility processes are counter-cyclical, persistent, and correlated with the mean of the endogenous variables.[6] As in Plagborg-Møller et al. (2020), we find a high degree of estimation uncertainty. However, despite the high estimation uncertainty, our approach based on a parametric model of stochastic volatility detects comovement between mean and volatility of macro and financial conditions. In addition, we find that estimation uncertainty is an important factor in shaping overall uncertainty and tail risk implied by the conditional densities.[7]

Section 4 presents the effects of structural shocks on uncertainty and tail risks, already summarized at the beginning of the introduction. Section 5 validates our model specification. The evolution over time of the measures of uncertainty and tail risk produced by our model compares well with alternatives from more flexible models such as Ludvigson et al. (2021)—who use a two-step approach originally developed in Jurado et al. (2015) based on factor models to measure financial and macroeconomic uncertainty—and Adrian et al. (2019), who use a two-step approach based on quantile regressions and parametric distributions to quantify risks to the GDP growth outlook. This section also shows the

---

[5]For instance, the quantile regressions in Adrian et al. (2019) are estimated with data on GDP growth and a financial factor; the Bayesian model in Plagborg-Møller et al. (2020) on GDP growth, a real factor and a financial factor.

[6]For financial variables, the correlation between first and second moments and the fact that this correlation can generate a fat left tail in conditional distributions, is known from the financial literature on the leverage effect (Bekaert and Wu, 2000), which includes Bayesian stochastic volatility models (Jacquier et al., 2004). The correlation between mean and volatility is also documented from macroeconomic data estimating factor models (Gorodnichenko and Ng, 2017). Aruoba et al. (2022) model a one-time shift in the mean and volatility of economic variables at the ZLB using a structural VAR.

[7]As in their analysis, we find that skewness and kurtosis of the densities do not show any sizeable movement. In this lively and growing literature, recent work by Delle Monache et al. (2021) finds evidence of time-varying skewness in the conditional distribution of future GDP growth.

robustness of our key results to alternative assumptions on shocks identification. Section 6 concludes the paper.

2 Econometric Framework and Identification Strategy

In this section, we first present a class of VAR models with stochastic volatility that allows for a rich interaction between mean and volatility. Then, we introduce a key object of interest, the conditional distribution, and discuss three key drivers of its fluctuations. We show how to compute impulse responses of uncertainty and tail risks from the conditional distribution. Next, we present the identification strategy used to identify macroeconomic and financial shocks. We conclude by providing some details about the data and the Bayesian estimation algorithm. Our model includes one real activity indicator and one financial indicator—real GDP growth and corporate credit spreads measured as the Baa corporate bond yield relative to the yield on 10-Year Treasuries—and two unobserved volatility processes associated with these variables.

2.1 Stochastic Volatility Vector Autoregressions

A reduced-form stochastic volatility (SV) VAR model describes the evolution of the endogenous variables z_t as follows:

$$z_t = c_z + \sum_{p=1}^{P} \beta_p z_{t-p} + \sum_{k=1}^{K} b_k h_{t-k} + H_t^{1/2} e_t, \tag{1}$$

$$h_t = c_h + \sum_{j=1}^{J} \theta_j h_{t-j} + \sum_{q=1}^{Q} d_q z_{t-q} + S^{1/2} \eta_t. \tag{2}$$

Equation (1) describes the evolution of z_t, an $N \times 1$ vector, which depends on an $N \times 1$ constant vector c_z, on lags of z_t, on lags of the unobserved $N \times 1$ vector of log volatility processes h_t, and on the $N \times 1$ vector of residuals e_t. The residuals feature time-varying volatility processes $\exp(h_t)$ collected in the $N \times N$ diagonal matrix H_t. Equation (2) describes the evolution of the volatility processes, which

depends on an $N \times 1$ constant vector c_h, on lags of h_t and z_t, and on an $N \times 1$ residual vector η_t. Equation (3) defines the distributions of the residuals e_t and η_t:

$$\varepsilon_t = \begin{pmatrix} e_t \\ \eta_t \end{pmatrix} \sim N(0, \Sigma), \quad \Sigma = \begin{pmatrix} \Sigma_e & \Sigma'_{e\eta} \\ \Sigma_{e\eta} & \Sigma_\eta \end{pmatrix}. \tag{3}$$

We follow Mumtaz (2018) and we assume that the time-invariant $2N \times 2N$ variance-covariance matrix Σ has diagonal elements normalized to 1 (as we have factored out the time-varying volatility) and the residuals e_t and η_t have a contemporaneous correlation $\Sigma_{e\eta}$. Thus, this model features endogenous volatility—as h_t can respond immediately to disturbances e_t and with delay to movements in z_t—and mean effects of volatility—as z_t can also respond immediately to disturbances in the volatility equation and with delay to movements in h_t.

To write the model in structural form, we define matrix A_0 such that $A'_0 A_0 = \Sigma$. The relationship between reduced-form residuals and structural shocks is:

$$\underbrace{\left(V_t^{1/2} A_0\right)^{-1}}_{B_{0,t}} \begin{pmatrix} z_t \\ h_t \end{pmatrix} = \nu_t, \; V_t = \begin{pmatrix} H_t & 0 \\ 0 & S \end{pmatrix}. \tag{4}$$

where ν_t denotes unit variance orthogonal structural shocks, $B_{0,t}$ is the matrix of contemporaneous structural coefficients and V_t is the variance of the reduced-form innovations. For computation purposes, we make the additional assumption that the structural coefficients are time invariant by fixing V_t to its deterministic steady state calculated by iterating the model for $1,000$ periods without shocks, so that $B_0 = \left(V_{ss}^{1/2} A_0\right)^{-1}$.

2.2 Measuring Nonlinear Effects of Shocks on Uncertainty and Tail Risk

The goal of our analysis is to study the nonlinear effects of structural shocks on uncertainty and risk about future outcomes. In this section, we describe the construction of uncertainty and tail risk responses to structural shocks. These responses are based on conditional distributions—hence are not the typical impulse response functions analyzed in VAR papers—and their use is key to our analysis as they fully

7

take into account model nonlinearities and all sources of model and estimation uncertainty.

Our approach involves two steps. In a first step, we compute a baseline conditional distribution $p(z_{t+1:t+f}|z^t)$:

$$p(z_{t+1:t+f}|z^t) = \int_\Theta \int_{H_t} \left[\int_{H_{t+1:t+f}} p(z_{t+1:t+f}, H_{t+1:t+f}|z^t, H_t, \Theta) dH_{t+1:t+f} \right] p(H_t|z^T, \Theta) p(\Theta|z^T) dH_t d\Theta.$$
(5)

At each point in time t, equation (5) describes the distribution of future values of all the endogenous variables through forecast horizon f, given current observable economic conditions z^t. The vector Θ collects the model parameters, including A_0, and z^T denotes the full sample of data used in estimation.

The conditional distribution includes the three relevant sources of uncertainty about future outcomes discussed in Geweke and Whiteman (2006) and Del Negro and Schorfheide (2013), among others: uncertainty regarding the future realization of the structural shocks ($p(z_{t+1:t+f}, H_{t+1:t+f}|z^t, H_t, \Theta)$), uncertainty about parameters of the model ($p(\Theta|z^T)$), and uncertainty about the unobserved volatility state ($p(H_t|z^T, \Theta)$).[8]

In a second step, we generate a counterfactual conditional distribution $p(z_{t+1:t+f}|z^t, \nu^*_{j,t+1})$, by assuming that a structural shock j materializes at time $t+1$. To construct the uncertainty and tail risk impulse responses to the structural shock $\nu^*_{j,t+1}$, we proceed by computing uncertainty and tail risk associated with the counterfactual and baseline distributions, and then take their differences.[9]

For variable z_i and horizon f, the uncertainty impulse response (UIR) is:

$$UIR_f[z_i|z^t, \nu^*_{j,t+1}] = U_f[z_i|z^t, \nu^*_{j,t+1}] - U_f[z_i|z^t],$$
(6)

where $U_f[z_i|z^t] = \sqrt{Var_t[z_{i,t+f}]}$ is the square root of the variance of the conditional distribution. This

---

[8]We estimate the model using the full sample of data z^T. Therefore, the latter two sources of uncertainty are both conditioned on z^T. The first source of uncertainty is given z^t conditions. This decomposition is akin to producing the smoothed estimate of the conditional distribution at time t, which we find appropriate given our interest in producing the best possible historical estimate of the conditional distribution at a point in time. We also suppress the conditioning on lags of H_t to save on notation in equation (5). We should be conditioning on all lags of H_t through $t+1-max\{J, K\}$.

[9]More precisely, as we discuss in the Appendix, we use *marginal* conditional distributions.

definition of uncertainty is used in many papers, including Orlik and Veldkamp (2014) and Jurado et al. (2015).

For variable z_i and horizon f, we compute tail risk as the location of the left tail of the conditional distribution—expected shortfall (ES)—and location of the right tail of the conditional distribution—expected longrise (LR).[10] Accordingly, the impulse responses are:

$$SFIR_f[z_i|z^t, \nu^*_{j,t+1}] = SF_f[z_i|z^t, \nu^*_{j,t+1}] - SF_f[z_i|z^t], \tag{7}$$

$$LRIR_f[z_i|z^t, \nu^*_{j,t+1}] = LR_f[z_i|z^t, \nu^*_{j,t+1}] - LR_f[z_i|z^t], \tag{8}$$

In our application, the impulse responses of shortfall and longrise for GDP growth—$SFIR_f[GDP]$ and $LRIR_f[GDP]$—represent the responses of downside and upside macroeconomic risks, respectively. These macroeconomic risk measures are closely related to the measures constructed by Adrian et al. (2019) to study GDP growth-at-risk. We complement the study of macroeconomic risk with new measures of financial risk, which we extract from corporate spreads. The shortfall and longrise measures for corporate credit spreads—$SFIR_f[CS]$ and $LRIR_f[CS]$—have the opposite interpretation. Shortfall in spreads represents upside financial risk, as the left tail of the spread distribution covers low level of spreads that typically reflect buoyant financial conditions. The longrise in spreads represents downside financial risk, as elevated levels of spreads represent tight financial conditions.

The presence of nonlinearities implies that we cannot calculate these impulse responses using standard formulas, as the dynamic response to a shock depends on the volatility states, the parameters of the model, and future values of the shocks. We employ simulation methods so that all of these dependencies are fully taken into account. The simulation algorithm is presented in the Appendix.

Our method to form impulse responses to uncertainty and tail risk is closely related to, but distinct from, Koop et al. (1996), which employs simulation methods to calculate impulse response functions (IRFs). IRFs compute the expected responses of the observables z_t to shocks conditional on the data,

---

[10]Formally, the expected shortfall is defined as $SF_f[z_i|z^t] = E_t[z_{i,t+f}|z_{i,t+f} < q_\alpha(z_{i,t+f})]$, while the expected longrise is defined as $LR_f[z_i|z^t] = E_t[z_{i,t+f}|z_{i,t+f} > q_{1-\alpha}(z_{i,t+f})]$. $q_{\alpha(z)}$ denotes the α-percent quantile of the distribution. Throughout the paper, we set $\alpha = 0.05$, thus considering the expected value in the bottom and top 5 % of the conditional distributions.

the volatility states, and the model parameters:[11]

$$IRF_f[z_i|z^t, H^t, \nu^*_{j,t+1}, \Theta] = E_f[z_i|z^t, H^t, \nu^*_{j,t+1}, \Theta] - E_f[z_i|z^t, H^t, \Theta]. \qquad (9)$$

IRFs are a useful tool to track the effects of shocks on model variables, and we employ it in Section 3 to illustrate key properties of our model. The notation in equation (9) emphasizes a crucial difference between IRFs and our responses UIR, SFIR, and LRIR. IRFs are model objects constructed conditioning on parameters and states. Hence, inference includes the construction of credible sets that reflect uncertainty about parameters and states. UIR, SFIR, and LRIR are constructed using conditional densities and *do not* condition on parameter and states, see equations (6)-(8). This is because conditional densities already factor in all sources of uncertainty.[12]

2.3   Identification of Shocks

Our identification scheme identifies two shocks that originate in the real economy and two shocks that originate in the financial sector.

Without loss of generality, we can assume that the first shock in the system is a macroeconomic shock and that the second shock is a financial shock. Accordingly, we can write the first two equations of the structural SV-VAR, abstracting away from lags, as:

$$z_{GDP,t} = \underbrace{\eta_{12}}_{<0} z_{CS,t} + \underbrace{\eta_{13}}_{(-1;1)} h_{GDP,t} + \underbrace{\eta_{14}}_{=0} h_{CS,t} + \nu_{M,t}, \qquad (10)$$

$$z_{CS,t} = \underbrace{\eta_{21}}_{<0} z_{GDP,t} + \underbrace{\eta_{23}}_{(-0.5;0.5)} h_{GDP,t} + \underbrace{\eta_{24}}_{=0} h_{CS,t} + \nu_{F,t}. \qquad (11)$$

Equations (10) and (11) are arranged so that, without loss of generality, real GDP growth and spreads are on the left hand side, respectively. The parameters η_{ij} are elasticities of real GDP growth and

---

[11]IRFs for the log volatility processes h_t can be computed using this same formula.

[12]An additional difference is related to the simulation algorithm used to compute the counterfactual distribution, discussed in the Appendix.

corporate spreads to contemporaneous movements in the other variables in the system.[13] Casting the model in terms of contemporaneous elasticities is convenient given their clear and simple economic interpretation. The underbraces display the restrictions on the elasticities discussed below.

The macroeconomic shock $\nu_{M,t}$ is a real activity shock that captures innovations in real GDP growth after controlling for the systematic response of GDP growth to movements in credit spreads and volatility. A real activity shock of this type is identified, for instance, in Ludvigson et al. (2021). The financial shock $\nu_{F,t}$ is a shock to credit spreads similar to Gilchrist and Zakrajšek (2012). As discussed throughout the paper, the high correlation between credit spreads and credit spread volatility is consistent with the notion that this shock captures exogenous movements in financial conditions that have simultaneously a first and second moment origin.

We then assume that the third and fourth shock originate from movements in volatilities not accounted for by the primary macroeconomic and financial shocks. Accordingly, and without loss of generality, we can write the third and fourth equations of the model as:

$$h_{GDP,t} = \underbrace{\eta_{31}}_{<0} z_{GDP,t} + \underbrace{\eta_{32}}_{>0} z_{CS,t} + \underbrace{\eta_{34}}_{=0} h_{CS,t} + \nu_{MV,t}, \tag{12}$$

$$h_{CS,t} = \eta_{41} z_{GDP,t} + \eta_{42} h_{GDP,t} + \eta_{43} h_{GDP,t} + \nu_{FV,t}. \tag{13}$$

The macroeconomic volatility shock $\nu_{MV,t}$ identifies variation in GDP growth volatility after accounting for the endogenous response of volatility to GDP growth and credit spreads. The financial volatility shock $\nu_{FV,t}$ plays only a modest role in our model, as we force it to explain only the variation in financial volatility unaccounted for by the other shocks. While the interpretation of the macro volatility shock is similar to the macroeconomic volatility shock identified in Ludvigson et al. (2021), the interpretation of the financial volatility shock is distinctly different. Ludvigson et al. (2021) do not include in the VAR credit spreads or other "level" indicators of financial conditions, so financial volatility is the only indicator capturing financial developments. Hence, in their model, the financial volatility shock likely

---

[13]The elasticities are transformations of the structural coefficients B_0. For example, $\eta_{12} = -b_{0,12}/b_{0,11}$ where $b_{0,11}$ and $b_{0,12}$ are the elements that multiply $z_{GDP,t}$ and $z_{CS,t}$ in the first row of B_0. We normalize the diagonal elements of B_0 to be positive.

plays the same role as our financial shock, capturing a broad set of shocks originating in the financial sector. We further discuss the interpretation of the financial shock in the robustness section.

The Identification Strategy

Our identification strategy imposes sign and zero restriction on the contemporaneous elasticities implied by the structural coefficients of the model. Our restrictions are motivated by results in widely-used DSGE models at the nexus between economic and financial conditions, and by findings shared across empirical studies of macroeconomic and financial volatility.

Restriction 1 (Relationship between GDP growth and spreads): *To identify the macro shock, the contemporaneous response of GDP growth to higher spreads is negative. To identify the financial shock, the contemporaneous response of corporate spreads to GDP growth is negative. That is, $\eta_{12} < 0$ in equation (10) and $\eta_{21} < 0$ in equation (11).*

Restriction 1 has two parts. First, all else equal, a tightening in financial conditions leads to lower economic activity. In theoretical models, as for instance Jermann and Quadrini (2012), adverse financial shocks reduce firms' capacity to finance investment, lowering growth. Second, higher economic activity lowers corporate spreads (Bernanke et al., 1999).

Restriction 2 (Impact of GDP growth volatility on mean): *To identify the macro and financial shocks, the contemporaneous responses of GDP growth and corporate credit spreads to GDP growth volatility are bounded: $\eta_{13} \in (-1; 1)$ in equation (10) and $\eta_{23} \in (-0.5; 0.5)$ in equation (11).*

There is a large body of literature documenting hump-shaped responses to macroeconomic uncertainty shocks. Typically, the impact response is muted, as for instance in Jurado et al. (2015). We select symmetric bounds around zero motivated by the theoretical literature on uncertainty. Theories of real option effects suggest a decline in real economic activity following an increase in volatility, while theories of growth options and Oi-Hartman-Abel effects suggest an expansion in activity (Bernanke, 1983; Bar-Ilan and Strange, 1996; Oi, 1961; Hartman, 1972; Abel, 1983).

We calibrate the bounds to allow for potentially sizeable impact effects of GDP growth volatility, while ruling out implausibly large effects. For real GDP growth, the bounds imply that a 20% increase in GDP growth volatility—corresponding to the standard deviation of its reduced-form innovation in

steady state—can lead up to a 0.2 percentage points change in GDP growth—which is about one-third of the steady state standard deviation of its reduced-form innovation of 0.7. For corporate credit spreads, the bounds imply that a 20% increase in GDP growth volatility can lead up to a 10 basis points change in spreads—which is about half of its innovation's steady state standard deviation of 0.19.

Restriction 3 (Endogenous component of GDP growth volatility): *The contemporaneous response of GDP growth volatility to higher GDP growth is negative and to higher spreads is positive. That is, $\eta_{31} < 0$ and $\eta_{32} > 0$.*

We impose that, all else equal, higher GDP growth reduces GDP growth volatility on average. This restriction is motivated by models that allow for changes in the speed of learning over the business cycle, which predict a negative relationship between economic activity and volatility (Van Nieuwerburgh and Veldkamp, 2006). In addition, higher borrowing costs make firm financing more difficult, which increases GDP growth volatility because the ability of firms to maintain production is hampered (Elenev et al., 2021).

Restriction 4 (Separating the financial and financial volatility shocks): *The contemporaneous response of GDP growth, corporate spreads and GDP growth volatility to spread volatility is zero. That is, η_{14}, η_{24} and η_{34} are 0.*

Restriction 4 assumes that financial developments are mediated, on impact, through the level of corporate credit spreads. The zero restrictions are imposed to discipline the structure of the financial block. As shown in the next section and a common finding in the literature, corporate credit spreads and spread volatility are highly correlated, making it hard to tease out the distinct effects of spreads and spread volatility (Caldara et al., 2016).[14]

Restriction 5 (Separating the macro and financial shocks): *The financial shock $\nu_{F,t}$ leads to a larger rise in corporate credit spreads contemporaneously than the macroeconomic shock $\nu_{M,t}$.*

We need to impose Restriction 5 to ensure that we can separately identify the macroeconomic and financial shock. In the Appendix, we show analytically that Restrictions 1 to 4 can identify all shocks with an exception, as there can be an identification problem between $\nu_{M,t}$ and $\nu_{F,t}$ that we solve by

---

[14]Some papers sidestep this identification challenge by including in empirical models either spreads or measures of financial volatility. For instance, Ludvigson et al. (2021) include in the VAR model only a measure of financial uncertainty.

imposing Restriction 5. In our application, we find that this last restriction is never binding, that is, the shocks identified by Restrictions 1 to 4 automatically satisfy it.

The main advantage of our approach is that it does not restrict the sign or size of the impulse responses and we leave unrestricted all remaining structural parameters of the model, so all shocks can potentially generate sizeable movements in macro and financial indicators. In addition, the restrictions we impose are compatible with a set of structural models rather than a unique one (Rubio-Ramirez et al., 2010; Arias et al., 2018).

2.4   Data, Estimation, and Model Specification

The model is estimated on data for U.S. real GDP growth and corporate credit spreads at quarterly frequency over the 1947:Q2-2019:Q4 sample.[15] We use corporate credit spreads because they are an important indicator of asset valuations, and spreads have emerged in empirical work as reliable and timely indicators of financial conditions (Gertler, 2012; Gilchrist and Zakrajšek, 2012).

In equation (1), we include 4 lags of the level variables and 2 lags of volatility. In the volatility equation (2), we include 1 lag of the volatility, and 2 lags of level variables. We use data from 1947:Q2 through 1953:Q1 as pre-sample to calibrate the prior distributions. We take $150,000$ draws from the posterior distribution, burn the first $50,000$, and sample every 25th draw to produce our posterior statistics of interest. Details about the prior distributions and the posterior sampler, as well as an estimation exercise on simulated data, are in the Appendix. Our implementation of the identification uses Algorithm 2 of Arias et al. (2018) to take independent draws from a distribution of structural models that conditions on the zero elasticity restrictions.[16]

---

[15]Data on GDP are from FRED. For corporate credit spreads, from 1947:Q2 through 1953:Q2, we take the difference between Moody's Seasoned Baa Corporate Bond Yield (BAA) and the 10-Year Treasury Constant Maturity Rate (DGS10). From 1953:Q3 onward, we use the Moody's Seasoned Baa Corporate Bond Yield Relative to the Yield on 10-Year Treasury Constant Maturity (BAA10Y). Quarterly values are calculated as averages of daily observations.

[16]As noted in Arias et al. (2018), Algorithm 2 is a valid identification strategy but inference might not be invariant to the order that the shocks are identified, a very unpalatable property. We verify that switching the order of shock identification does not materially alter the results. In addition, the posterior distribution over the structural parameterization is not of the normal generalized normal form as in Arias et al. (2018) and it requires simulation methods to draw from its posterior, as our model is not linear. Therefore, step 1 in our implementation of Algorithm 2 uses a draw from our estimation algorithm.

Figure 2: Volatility of GDP Growth and Corporate Spread Innovations Move Significantly Over Time
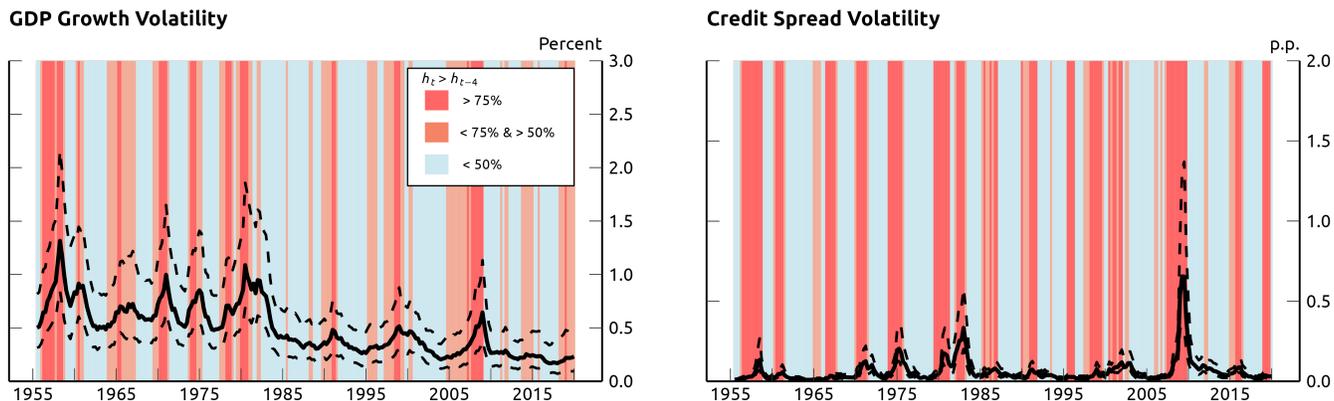
NOTE: The figure plots the evolution of the estimated volatility processes for GDP growth and corporate spreads, corresponding to the diagonal elements of H_t. The solid black lines are the pointwise median estimates of the posterior distribution, whereas the dashed lines are the pointwise 10th and 90th percentiles. The light blue shaded areas denote the time periods in which the percentage of posterior draws that imply $h_t > h_{t-4}$ is less than 50%. The light red areas are times when this percentage is between 50% and 75% and the dark red areas are when the percentage is above 75%.

3   Model Estimates

In this section, we examine three sets of model estimates that contribute to shaping the response of uncertainty and tail risk to the structural shocks. First, we show the model estimates of the volatility processes. Second, we show estimation results of the model parameters. Third, we discuss the impulse responses of model variables to structural shocks, showing how the effects are state-dependent.

3.1   Volatility Processes

The solid lines in Figure 2 show the median estimates of GDP growth and spread volatility, which are the unobserved volatility processes for GDP growth and corporate spreads in matrix H_t, expressed in percent GDP growth and percentage points of spreads, respectively. These objects are distinct from GDP growth and spread uncertainty, which are calculated from the standard deviations of the conditional distributions. The dashed lines represent the corresponding 80-percent pointwise credible bands. To understand the extent of time variation of the volatility processes implied by the model, we calculate the posterior probability of volatility at time t being higher than four quarters earlier. Red

15

Table 1: MODEL ESTIMATES OF KEY PARAMETERS

Parameters	Contemporaneous $\Sigma^{e_{GDP},e_{CS},\eta_{GDP},\eta_{CS}}$	Persistence $\beta_1^{GDP,CS}$ $\qquad$ $\theta_1^{h_{GDP},h_{CS}}$	Lag Vol on Level $b_{1,CS,h_{CS}}$	Lag Level on Vol $d_{1,h_{GDP},CS}$ $\quad$ $d_{2,h_{GDP},CS}$ $\quad$ $d_{1,h_{CS},GDP}$
Median	$\begin{pmatrix} 1 & & & \\ -0.34^* & 1 & & \\ -0.27 & 0.19 & 1 & \\ -0.41^* & 0.66^* & 0.40 & 1 \end{pmatrix}$	$\begin{pmatrix} 0.28^* & -0.47^* \\ -0.01^* & 0.90^* \end{pmatrix} \begin{pmatrix} 0.70^* & 0.21^* \\ -0.01 & 0.88^* \end{pmatrix}$	0.14^*	-0.03^* $\qquad$ -0.03^* $\qquad$ -0.15^*

NOTE: "Contemporaneous" shows the contemporaneous correlation matrix of the innovations. "Persistence" shows the first order lag matrix in the VAR for the level variables (β_1) and volatility variables (θ_1) as described in equations (1) and (2). The superscripts of the parameters indicate the order of the variables. "Lag Vol on Level" shows the first order lag of volatilities on level variables. "Lag Level on Vol" shows the first order lag of level variables on volatilities. The subscripts of the parameters index the coefficient, with the first term denoting the lag order, the second term denoting the left hand side variable in the regression, and the third term denoting the right hand side variable. * denotes significance at the 80% credible set level.

shadings denotes quarters with a probability higher than 0.75.[17]

The volatility processes display four distinct features. First, GDP growth and spread volatility are both counter-cyclical, see for example the early 1980s and 2008-2009 recessions, with GDP growth volatility having a smaller negative correlation with GDP growth (-0.16) than spread volatility (-0.34). Second, spread volatility is highly correlated with corporate spreads (0.72, not shown). On the one hand, this high correlation will turn out to be an important driver of uncertainty and tail risk. On the other, the correlation makes it hard to identify two distinct financial shocks, and it is the basis for Restriction 4 in our identification strategy. Third, estimation uncertainty is large for GDP growth volatility—in line with findings in Plagborg-Møller et al. (2020)—and low for spread volatility, as shown by the broken lines in the figure. Fourth, even though estimation uncertainty goes up in recessions (as calculated using pointwise credible bands), we find strong evidence of time variation in both volatility processes, especially of rises around recessions. Using the probability of volatility being higher than the previous year, the intensity of which is measured by the shading in the figure, we find evidence of rising GDP growth volatility in the late 1950s, with the probability peaking at 0.90 in 1958:Q2. This pattern materializes again during the global financial crisis (GFC), with the probability peaking at 0.88 in 2008:Q1. The post-GFC decline in volatility is as dramatic, with only a 0.02 probability of volatility being higher than the year before in 2009:Q4, that is, a 0.98 probability of a decline in volatility.

---

[17]While pointwise credible sets are useful to gauge estimation uncertainty in a given period, they are less useful to compare volatility estimates across time as the comparison does not happen draw by draw.

3.2 Reduced-Form Parameters

Table 1 displays the posterior estimates of the parameters governing the relationship between the endogenous variables and the volatility processes. The first column reports the contemporaneous correlations between level and volatility innovations in the model. The median correlation between innovations in GDP growth and GDP growth volatility is -0.27, while the median correlation between innovations in spreads and spread volatility is 0.66. There is evidence of contemporaneous cross correlations between GDP growth and spread conditions, with a correlation of -0.34 between GDP growth and spread level innovations and -0.41 between GDP growth and spread volatility innovations.

The remaining three columns report posterior estimates of the parameters generating dynamic correlations between the endogenous variables and volatility processes. Estimates reported in the second column show that the model generates persistent dynamics for the endogenous variables and the volatility processes. Persistence arises through coefficients on their own lagged values (for instance corporate spreads are highly persistent, with a 0.9 estimated coefficient) and on cross lags (for instance current GDP growth volatility being positively related to past spread volatility, with a 0.21 estimated coefficient). Estimates reported in the third column show that lagged volatility impact the endogenous variables—for instance, lagged spread volatility increases the level of spreads in the current quarter— while estimates reported in the last column show that lagged endogenous variables impact volatility—for instance, lower lagged spreads predict higher contemporaneous GDP growth volatility and lower lagged GDP growth raises current spread volatility.

In summary, three results emerge from the analysis of the volatility and parameter estimates. First, GDP growth and spread volatility processes display significant time variation and are correlated with the level of the endogenous variables. Second, there is persistence both in the level and volatility of the endogenous variables. Third, there is a rich cross-correlation structure between GDP growth and spread conditions and across level and volatility processes. These features of the model play an important role in understanding the impulse responses to the structural shocks discussed next.

Figure 3: IMPULSE RESPONSE FUNCTIONS (IRFs) IN HIGH AND LOW VOLATILITY STATES
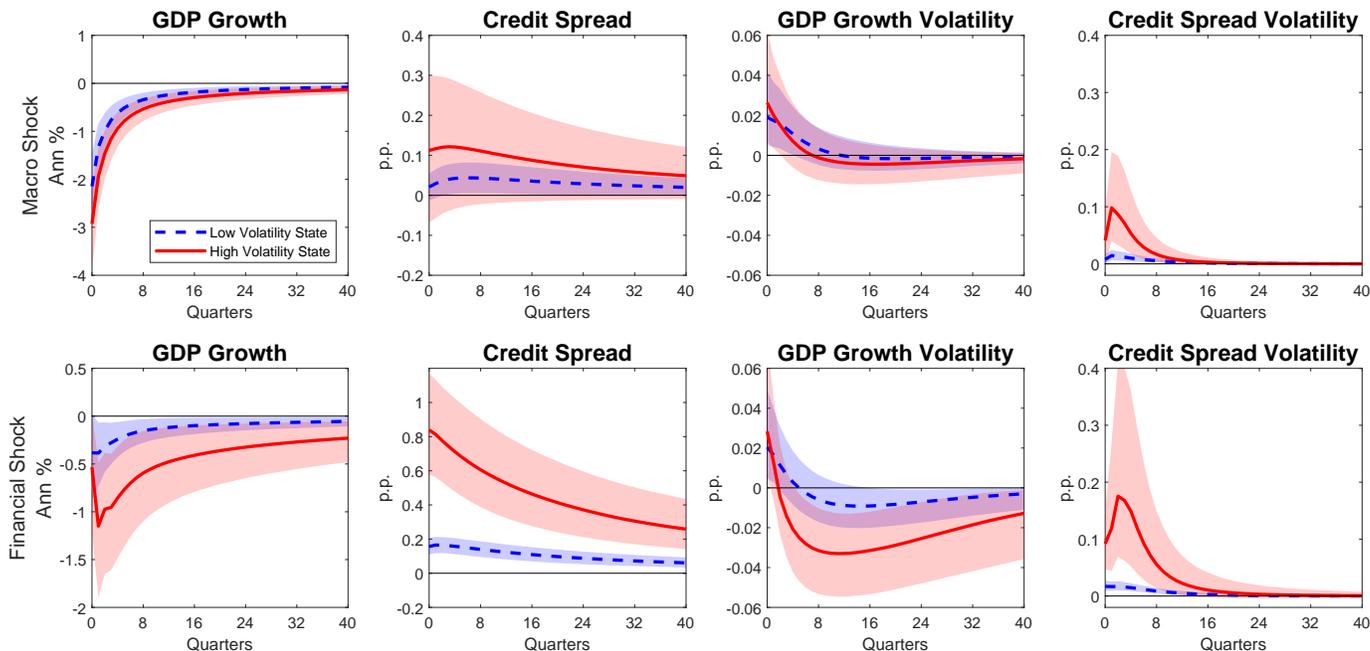
(a) Impulse Response Functions
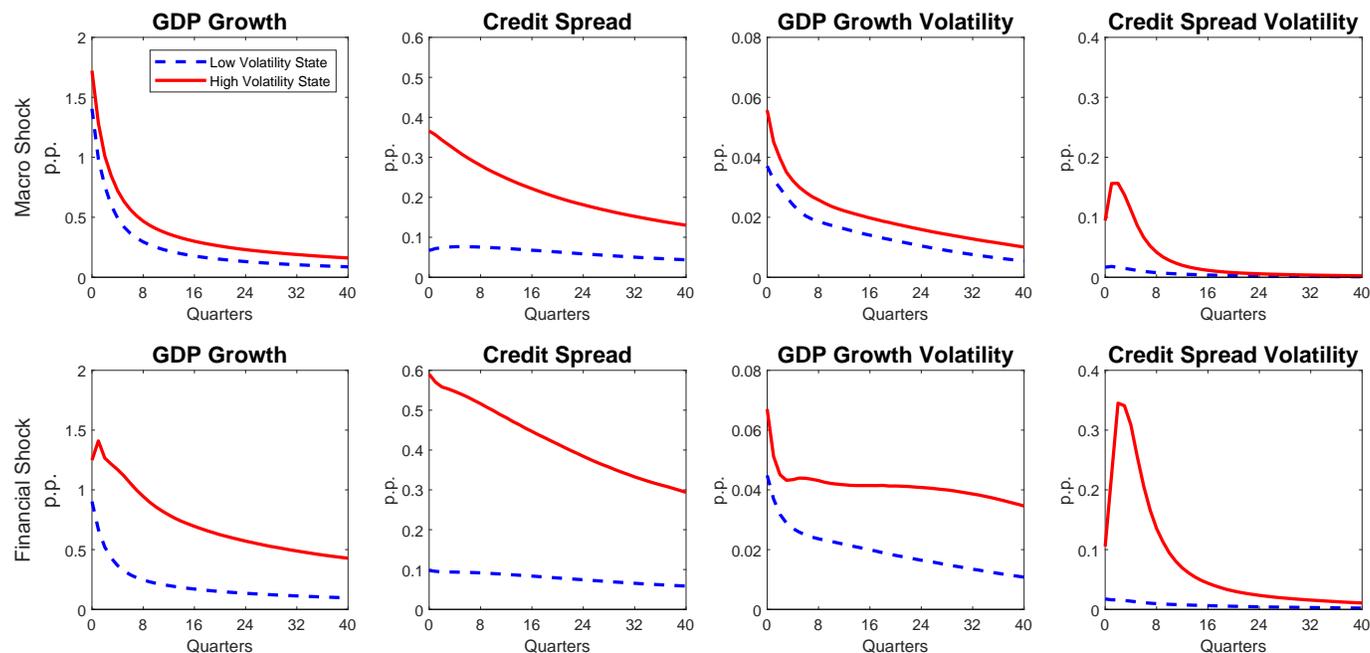
(b) IRFs: Width of Credible Sets

NOTE: The red (blue) lines in the top panel depict the median impulse responses to a one standard deviation macro and financial shock conditioning on 2008:Q4 (2006:Q4), a quarter of high (low) volatility. Shaded areas denote 80 percent credible sets. The volatility responses of the reduced form innovations are in percentage points. The bottom panel depict the width of the 80 percent credible set of the corresponding impulse responses plotted in the top panel. The width of credible sets are all reported in percentage points.

18

3.3 Impulse Response Functions

Panel (a) of Figure 3 plots the impulse responses defined in equation (9) to a one standard deviation adverse macroeconomic shock $\nu_{M,t}$ and adverse financial shock $\nu_{F,t}$. The GDP growth responses show annualized average GDP growth between horizon 1 and f, where f denotes the forecast horizon. The spread responses are the average spreads in percentage points between horizon 1 and f. The blue dashed lines plot median responses conditioning on 2006:Q4 data, a quarter characterized by low volatility, while the red solid lines plot median responses conditioning on 2008:Q4 data, a quarter characterized by high volatility. The shaded areas are 80 percent credible sets reflecting uncertainty around volatility states and model parameters.

Both shocks—irrespective of the conditioning state—generate business cycle correlations among the variables in the model: GDP growth declines while corporate spreads and the volatility processes rise. The increase in GDP growth volatility is short-lived, while the response of the remaining variables is persistent. The effects of both shocks is larger in periods of high volatility, but the amplification generated by the high volatility state is stronger for financial shocks than for macro shocks. The GDP growth response to a financial shock is tripled after 4 quarters while the spread response is quadrupled on impact. The volatility state also alters the propagation of shocks. Most notably, financial shocks induce a larger reversal in GDP growth volatility when volatility is high, despite inducing a similar impact response for low and high volatility states.[18]

Panel (b) of Figure 3 plots the width of the credible sets of the IRFs to macroeconomic and financial shocks reported in panel (a), that is, the uncertainty around the economic effects of these shocks. Such uncertainty is large: for all variables, the width of the credible set is of a size comparable to the response itself. In addition, the width of the credible set depends on the conditioning state, as high volatility states greatly amplify uncertainty surrounding the effects of both macro and financial shocks.

In the Appendix, we plot the IRFs associated with the macroeconomic volatility shock $\nu_{MV,t}$ and financial volatility shock $\nu_{F,t}$. We find that these shocks do not generate business cycle correlations, as they do not generate movements in GDP growth and corporate credit spreads. By contrast, these two shocks can generate sizeable movements in volatility. It is important to stress that our identification

---

[18]This volatility reversal of GDP growth aligns with findings in Adrian et al. (2022).

strategy does not impose zero restrictions on impulse responses nor restrictions on dynamic responses. Hence, this result is an outcome of the estimation. For the financial volatility shock our findings are not surprising: as mentioned, corporate credit spreads and spread volatility are highly correlated, and it turns out that the two main macro and financial shocks account almost entirely for their correlation, a result further examined in the robustness section.

# 4   The Effects of Shocks on Uncertainty and Tail Risk

With the groundwork laid out in the previous sections, we are now in a position to discuss the effects of macro and financial shocks on conditional distributions. We first show the effects of adverse macro and financial shocks on GDP growth and spread uncertainty and tail risk given 2008:Q4 conditions. Then, we parse out these effects in terms of the contribution of conditional mean and volatility changes, parameter and state uncertainty, and the higher-order effect. With all three channels active, we find that an adverse shock has a larger effect on GDP growth and spread uncertainty compared to a good shock, suggesting the presence of asymmetries in the responses of the conditional distributions to a shock.

4.1   Responses to Bad Shocks

In response to macroeconomic and financial shocks, GDP growth and spread uncertainty and downside risk of adverse events increase, while the upside risk of favorable events does not respond as much. Figure 4 illustrates this result, showing the uncertainty, shortfall, and longrise impulse responses (UIR, SFIR, and LRIR described in Section 2) to one standard deviation adverse macroeconomic and financial shocks conditioning on 2008:Q4 conditions.

While both shocks drive uncertainty and risk, their relative importance varies across horizons. The relative impact of macroeconomic shocks is largest within the first year, while financial shocks play a dominant role at longer horizons. For instance, on impact, the response of GDP growth uncertainty is over 40 percent *higher* to a macro shock than to a financial shock (0.36 vs. 0.25 percentage points). At horizon 12, however, the response of GDP growth uncertainty is 50 percent *smaller* to a macro shock

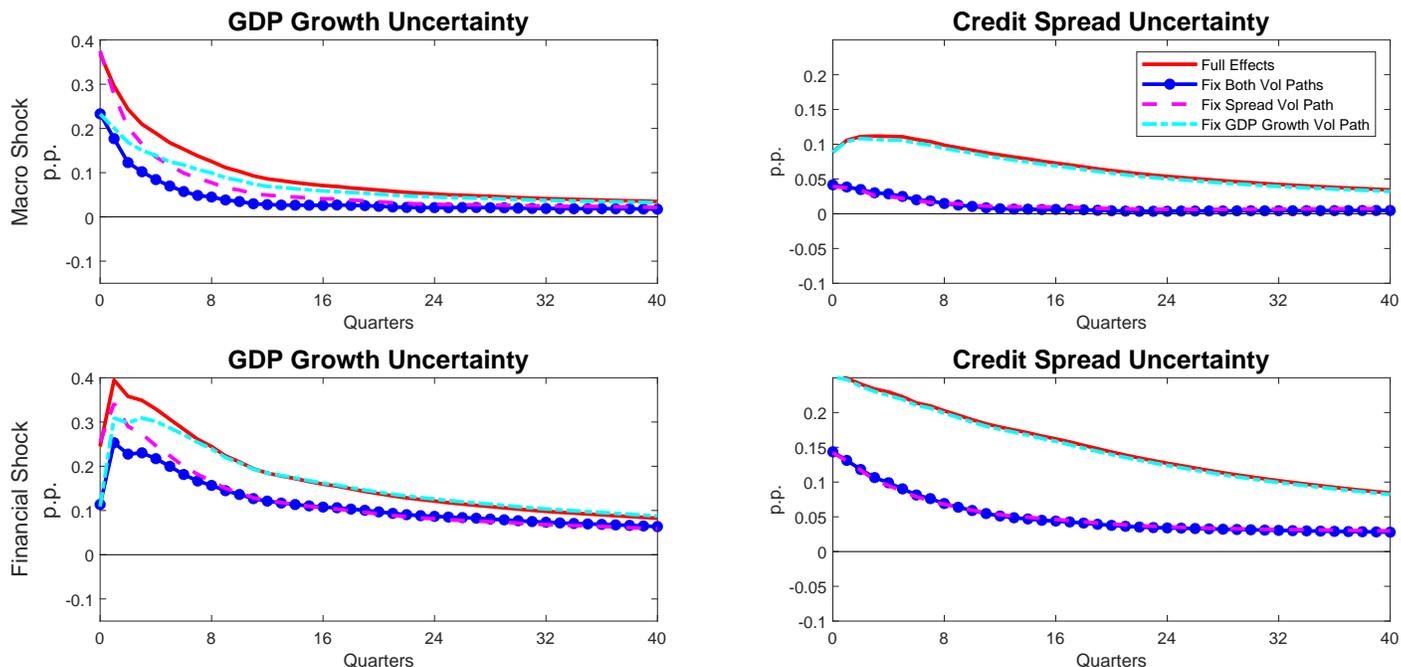Figure 4: THE RESPONSE OF UNCERTAINTY AND TAIL RISK TO SHOCKS
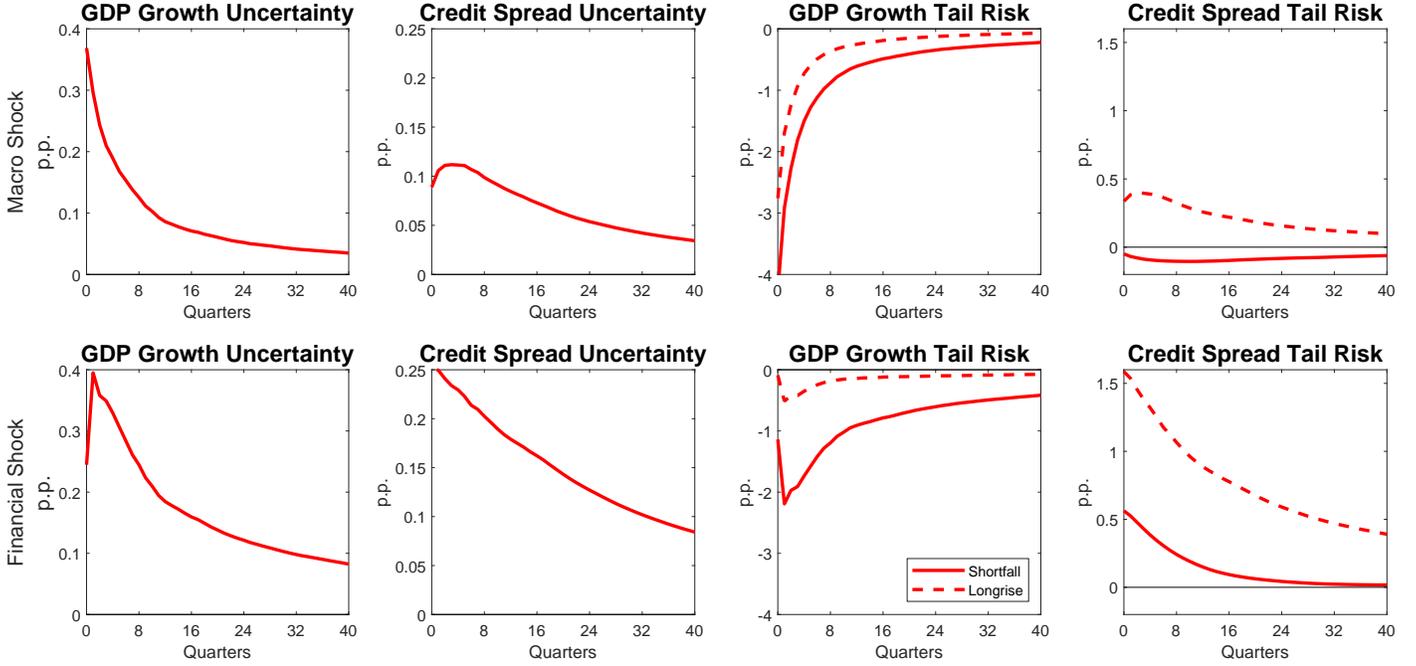
NOTE: The figure plots the responses of GDP growth and spread uncertainty and tail risk to a one standard deviation adverse macro (top row) and financial shock (bottom row) conditioning on 2008:Q4 data and volatility. GDP growth uncertainty and tail risk are computed from conditional densities of annualized average GDP growth between horizon 1 and f, where f denotes the forecast horizon. Similarly, spread uncertainty and tail risk are computed from conditional densities of average spreads between horizon 1 and f when calculating spread uncertainty and tail risk. All impulse responses are reported in percentage points.

(0.09 vs. 0.18 percentage points). Other measures of uncertainty and risk follow a similar pattern.

Figure 4 also reveals the importance of tracking the effects of shocks on both uncertainty and measures of tail risk. The tails capturing adverse risks (the left tail of the GDP growth distribution—measured by the shortfall—and the right tail of the spread distribution—measured by the longrise) move by more than the tails measuring upside risks (the right tail of the GDP growth distribution—measured by the longrise—and the left tail of the spreads distribution—measured by the shortfall). For instance, after an adverse macro shock, GDP growth tail risk falls, with the shortfall declining by 4 percentage points and the longrise falling by less than 3. This result follows from the fact that shocks in our model generate a simultaneous shift in the mean and uncertainty of the conditional distributions through the mechanisms illustrated by the impulse response functions in Section 3.3. If shocks were moving only the mean of the conditional densities, shortfall and longrise would shift in parallel. If shocks were moving only uncertainty, shortfall and longrise would move by the same amount but in opposite directions.

21

Figure 5: The Volatility Channel: How the Volatility of GDP Growth and Corporate Spread Innovations Move

NOTE: The figure plots the responses of GDP growth and spread uncertainty to a one standard deviation adverse macro (top row) and financial shock (bottom row) assuming 2008:Q4 data and volatility state. The solid red line is the baseline response in the full model. We consider three alternatives in which (i) we do not allow GDP growth and spread volatility to respond to the shocks (blue line with dots); (ii) we do not allow GDP growth volatility to respond to shocks (dot dashed cyan line); (iii) we do not allow spread volatility to respond to shocks (dashed magenta line). All impulse responses are reported in percentage points.

4.2   The Three Channels of Shock Propagation to Uncertainty and Risk

There are three channels that enable structural shocks in the model to move uncertainty and risk: a volatility channel; an estimation uncertainty channel; and a "higher-order" channel operating through the interaction between structural shocks and time-varying volatility in the baseline distribution.

The volatility channel operates through the effects of shocks on the volatility of the innovations, which alters the evolution of $p(z_{t+1:t+f}, H_{t+1:t+f}|z^t, H_t, \Theta)$ in the conditional densities as can be seen in equation (5). Time-varying volatility and correlation between mean and volatility play important roles in how the model generates time-varying uncertainty and growth-at-risk.[19]

Figure 5 shows that the volatility channel plays a prominent role in shaping the effects of the

---

[19]Note again that volatility refers to the volatility of the GDP growth and spread innovations while uncertainty refers to the standard deviation of the GDP growth and spread conditional distributions.

structural shocks for uncertainty (we omit the response of tail risk for exposition purposes). When the channel is not at play (the blue lines with dots), in other words, GDP growth and spread volatility are both not allowed to respond to shocks, the effects of a financial shock on GDP growth uncertainty after two years is over 30 percent lower and on spread uncertainty is 67 percent lower. Simulations that fix only one volatility process at a time reveal that GDP growth and spread volatility both matter for GDP growth uncertainty, while GDP growth volatility is not an important driver of spread uncertainty. The importance of spread volatility for GDP growth uncertainty is a result of the parameter estimates discussed in Section 3. There is a strong relationship between past spreads and present GDP growth. Therefore, if the volatility of spreads decreases, this naturally has an effect on the distribution of GDP growth with a lag.

The estimation uncertainty channel operates through uncertainty surrounding model parameters and volatility states. Estimation uncertainty translates into uncertainty on the effects of shocks, which alters the evolution of the posterior density through the terms $p(\Theta|z^T)$ and $p(H_t|z^T, \Theta)$. This channel can be of quantitative relevance because, as shown in Sections 3.1 and 3.2, there is a substantial amount of estimation uncertainty around model parameters and volatility states, especially in recessions.

Figure 6 illustrates how the estimation uncertainty channel injects randomness into the conditional distribution contributing to shape GDP growth and spread uncertainty. Each of the 100 thin blue lines in the figure depicts the response of uncertainty computed by fixing the parameters and the states of the model to different draws from the posterior distribution. The higher the estimation uncertainty, the larger the dispersion of the uncertainty measures produced by otherwise identical one standard deviation shocks. The importance of the estimation uncertainty channel is largest at short horizons, when shocks have their largest effects. Our preferred measure of uncertainty, reported in red, appropriately integrates over these responses in a way consistent with the posterior distribution.

The higher-order channel operates through the interaction between structural shocks and time-varying volatility in the baseline distribution. This channel is distinct from the volatility channel as it does not operate through the direct effects of shocks on the volatility processes. Instead, the impacts of shocks differ depending on from where they jump off in the baseline distribution. If the correlation between level and volatility in the baseline distribution is positive as is the case for corporate spreads,

Figure 6: THE ESTIMATION UNCERTAINTY CHANNEL OF THE RESPONSES IS SUBSTANTIAL
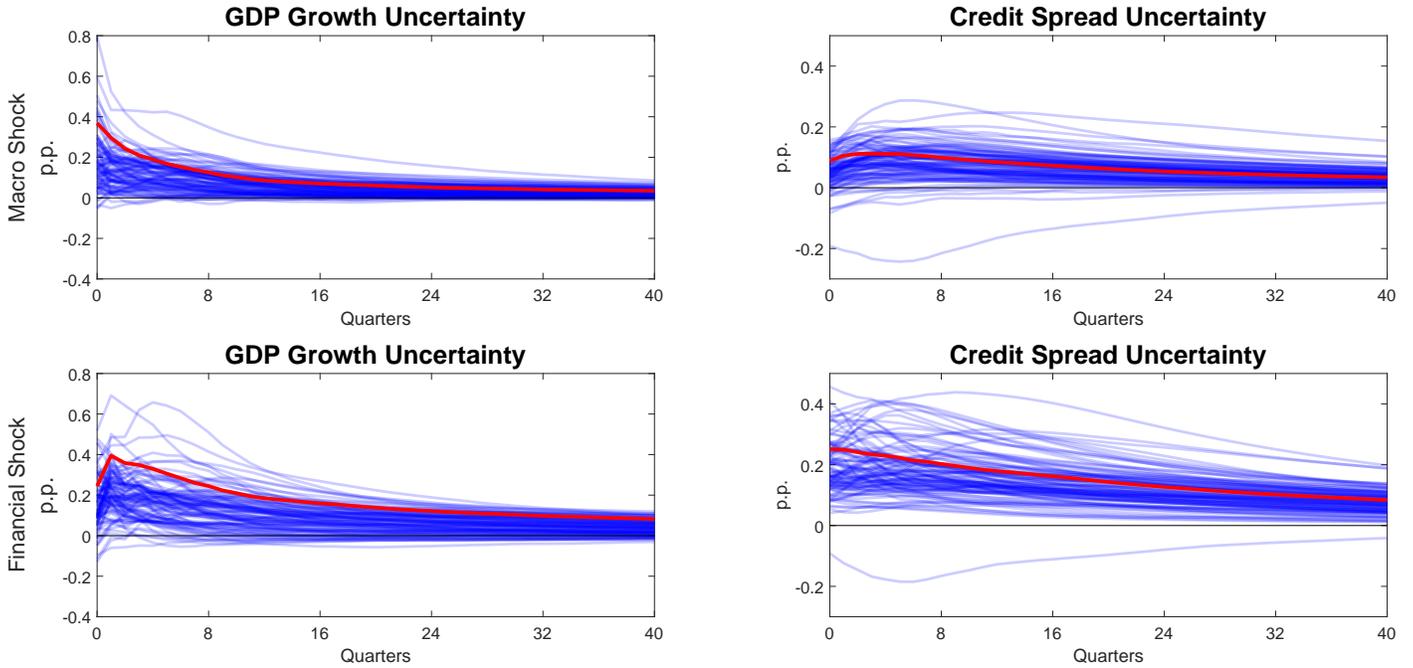
NOTE: The figure plots the responses of GDP growth and spread uncertainty to a one standard deviation adverse macro (top row) and financial shock (bottom row) assuming 2008:Q4 data and volatility state. The solid red line is the baseline response in the full model. Each of the 100 thin blue lines show responses conditional on a draw from the posterior distribution of the structural parameters and volatility states. All impulse responses are reported in percentage points.

then adverse shocks starting from the right tail of the distribution have larger impacts relative to those starting from the left tail.

Figure 7 illustrates how the higher-order channel injects randomness into the conditional distributions. Each of the 100 thin blue lines in the figure depicts the response of uncertainty computed by fixing the parameters and the states of the model to different draws from the posterior distribution, and shutting down the response of the volatility processes to the structural shocks. The response of GDP growth and spread uncertainty still move, indicating that the conditional distributions change. This effect comes uniquely from the higher-order channel, as the other two channels are not operative.

4.3   Asymmetric Effects of Bad versus Good Shocks

We close the section by comparing the effects of bad versus good shocks on uncertainty, which is shown in Figure 8. In our model, a one standard deviation adverse shock, which is shown in red, raises GDP

Figure 7: THE HIGHER-ORDER CHANNEL: UNCERTAINTY DYNAMICS WITHOUT VOLATILITY
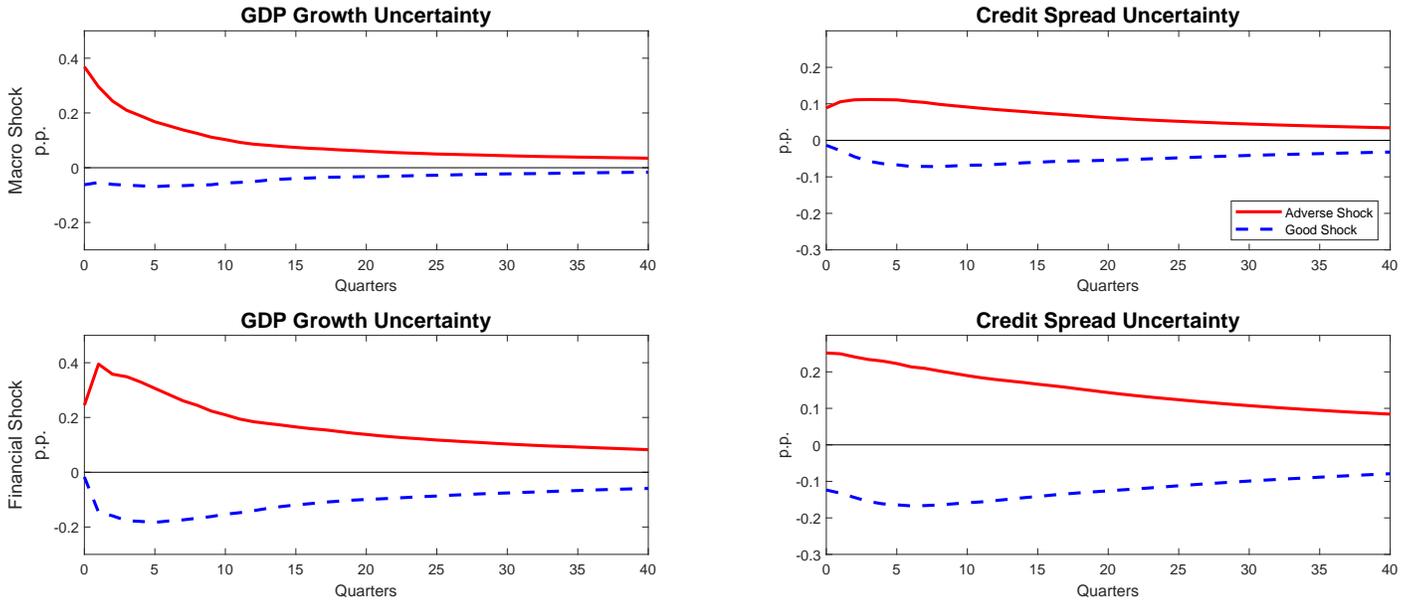CHANGES OR ESTIMATION UNCERTAINTY
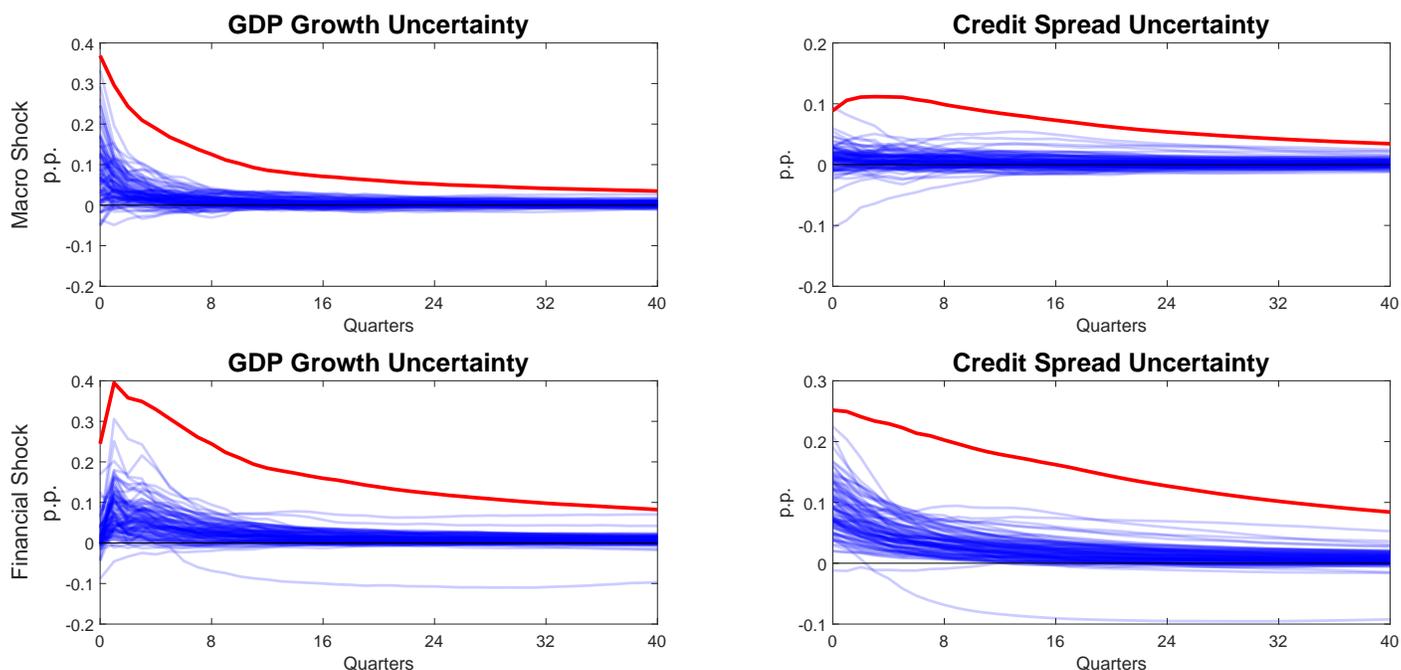
NOTE: The figure plots the responses of GDP growth and spread uncertainty to a one standard deviation adverse macro (top row) and financial shock (bottom row) assuming 2008:Q4 data and volatility state. The solid red line is the baseline response in the full model. Each of the 100 thin blue lines show responses conditional on a draw from the posterior distribution of the structural parameters and volatility states, with only the higher-order effect active. All impulse responses are reported in percentage points.

growth and spread uncertainty more than a one standard deviation good shock, which is shown in dashed blue, lowers them. In other words, a shock in our model has asymmetric effects on uncertainty. There are two main reasons for this behavior. First, we model the volatility processes in logs, as is standard in the literature (Clark, 2011). Shocks that move log volatility symmetrically have asymmetric effects on uncertainty. Second, estimation uncertainty increases overall uncertainty no matter whether the shock is positive or negative. This channel amplifies the effects of adverse shocks that raise uncertainty while muting the effects of good shocks that lower it.

5 Model Validation and Robustness

In this section, we validate our model estimates of uncertainty and risk by comparing them to two popular measures in the literature, Ludvigson et al. (2021) and Adrian et al. (2019). Then, we show

25

Figure 8: Bad Shocks Have Larger Effects than Good Shocks Do

NOTE: The solid red (dashed blue) lines in the figure plot the responses of GDP growth and spread uncertainty to a one standard deviation bad (good) macro and financial shock assuming 2008:Q4 data and volatility state. All impulse responses are reported in percentage points.

robustness to our identifying assumption that financial effects are mediated through spreads.

5.1 Time Series Measures of Uncertainty and Tail Risk

We can use our model to extract the historical behavior of GDP growth and spread uncertainty and tail risk. To do so, we compute conditional distributions for GDP growth and corporate spreads one quarter ahead. We then extract the uncertainty and 5% tail risk measures defined in Section 2. Our measures are reminiscent of indicators that have been developed in the literature on uncertainty and growth-at-risk. We therefore also compare our versions of uncertainty and risk with measures from two widely cited papers in the literature: (1) Ludvigson et al. (2021) for macroeconomic and financial uncertainty, and (2) Adrian et al. (2019) for GDP growth risk—henceforth LMN and ABG, respectively.

Figure 9 shows in red the one quarter ahead GDP growth and spread uncertainty in the top row and the one quarter ahead GDP growth and spread tail risk in the bottom row produced by the SV-VAR model. The measures of GDP growth and spread uncertainty are characterized by a clear pattern of

Figure 9: Uncertainty and Risk Measures:
Comparison with Adrian et al. (2019) and Ludvigson et al. (2021)
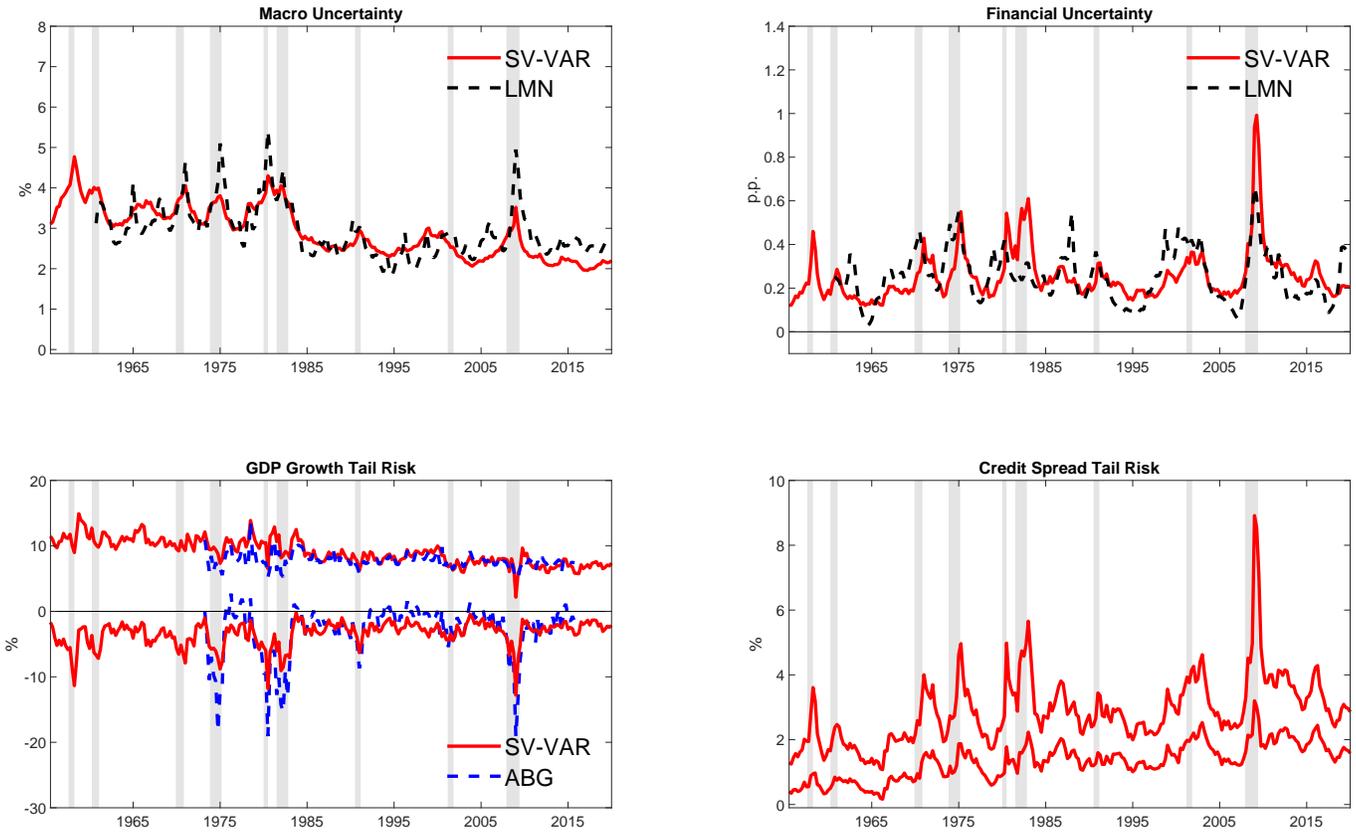
NOTE: The upper panels plot our estimates of one-quarter ahead GDP growth and spread uncertainty (solid red lines) and the quarterly average of the three month ahead real and financial uncertainty measures from Ludvigson et al. (2021) (dashed black lines), standardized to have the same sample mean and standard deviation as our uncertainty series. The lower panels plot our estimates of one quarter ahead (left panel) GDP growth tail risk (solid red lines) against estimates of GDP growth tail risk from Adrian et al. (2019). The right panel plots one quarter ahead spread tail risk. Gray shaded areas are recession dates as defined by the National Bureau of Economic Research.

cyclical variation, being negatively correlated with expected GDP growth and positively correlated with expected financial conditions. They spike during recessions and then slowly ease afterwards, which is consistent with the asymmetric effects on uncertainty of adverse versus good shocks documented in Section 4. The second row shows GDP growth and spread shortfall and longrise. GDP growth shortfall is especially volatile in recessions, whereas GDP growth longrise is more stable. The GFC features large declines in the shortfall, but not unprecedentedly so compared to the historical record. Spread longrise also spikes during recessions, consistent with the spike in spread uncertainty. In contrast with the behavior of GDP growth shortfall, the GFC has the largest spike on record in the spread longrise,

highlighting the important role that tight financial conditions played in the crisis.

The dashed black lines in the figure show the macro and financial uncertainty series of LMN and the dashed blue lines show the GDP growth tail risk series of ABG for comparison. Despite the varying data and methodologies used, our measures of uncertainty and tail risk largely cohere with those in the literature. The correlation between macroeconomic uncertainty measures is about 0.8, and the two measures share major spikes. The correlation between the financial uncertainties is lower, standing at 0.6. The measures share only some spikes—during the 1970s and during the GFC—while differing in the 1980s and 1990s. The difference, in part, reflects the choice of underlying financial variables. We use corporate credit spreads, while the LMN measure mostly loads on stock returns. As a result, for example, our spread volatility measure does not spike during the stock market crash of October 1987 while the LMN measure does. Turning to GDP growth tail risk, the correlation between shortfall measures is around 0.9 at the one quarter horizon. The correlation for the longrise is lower, at 0.7 one quarter ahead, although the two models share some spikes.

## 5.2 Alternative Zero Restrictions on Financial Variables.

In this robustness exercise, we assume that the effects of financial shocks are mediated through spread volatility instead of spreads. In Restrictions 1-3 and 5, we replace all of the elasticity restrictions that involve corporate spreads with spread volatility, keeping the signs and magnitudes of the restrictions the same.[20] In Restriction 4, we assume instead that the contemporaneous response of economic activity, corporate spreads, and GDP growth volatility to spreads is zero.

Figure 10 confirms that this alternative specification of the identification restrictions yields very similar impulse responses. Responses to the macro shocks are nearly identical, while responses to the financial shocks are slightly attenuated, in particular the response of corporate spreads to the shock. This is intuitive and reassuring, as the correlation between spreads and spread volatility is high (0.7), but there is some independent variation.

---

[20]In Restriction 2, the fraction of the total standard deviation of spread volatility that the GDP growth volatility shock is allowed to explain is around 30%. This compares to around 50% of spread innovation standard deviation in our benchmark identification because the standard deviation of spread volatility innovations is higher than those of spreads.

Figure 10: IMPULSE RESPONSES - ALTERNATIVE MODEL SPECIFICATIONS
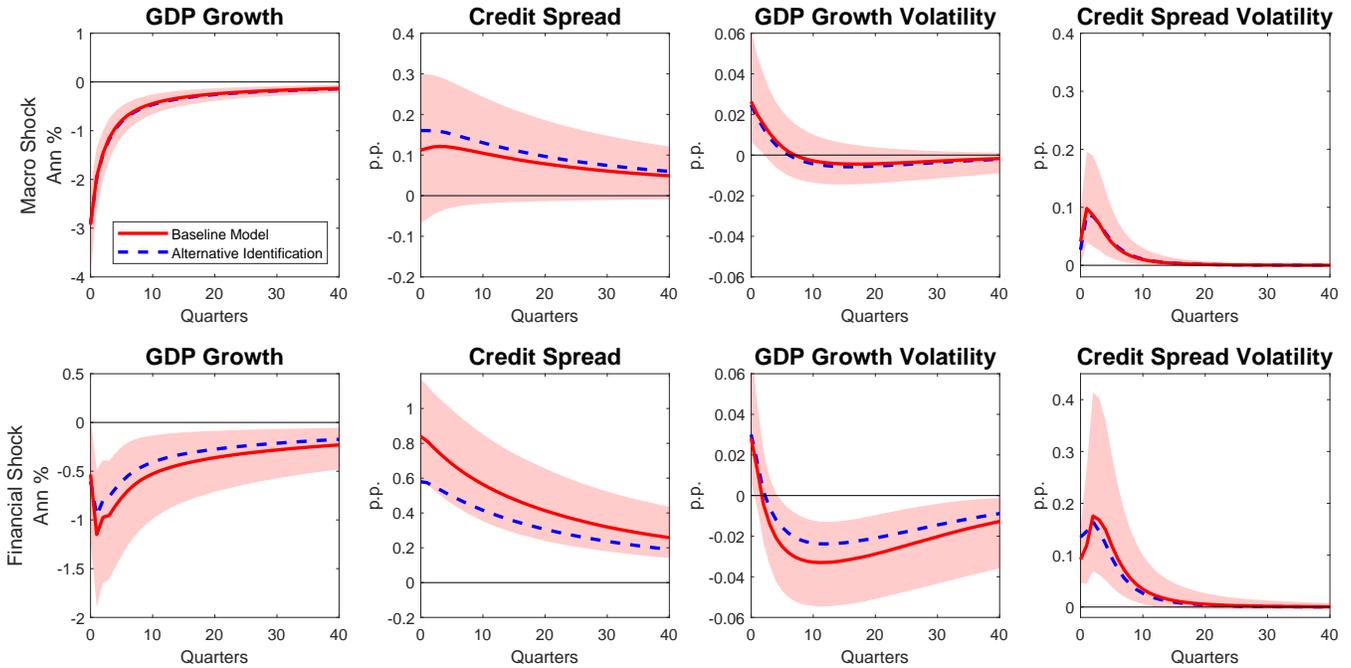
NOTE: The red lines depict the median impulse responses to a one standard deviation macro and financial shock conditioning on 2008:Q4, a quarter of high volatility. Shaded areas denote 80 percent credible sets. The volatility responses of the reduced form innovations are in percentage points. The blue dashed lines depict median impulse responses from the alternative identification strategy described in the main text.

6 Conclusions

The paper presents a unified framework that analyzes uncertainty and tail risk around economic and financial forecasts using a SV-VAR model estimated with Bayesian methods. By imposing sign and zero restrictions on the structural parameters of the model, the paper identifies macro and financial shocks that move uncertainty and risk. The results show that adverse shocks generate an increase in uncertainty and downside tail risk for future GDP growth and financial conditions. Macroeconomic shocks have a significant impact on uncertainty and downside risk at shorter horizons, while financial shocks account for most of the variation at longer horizons.

In the analysis presented in the paper, we have considered macro and financial shocks in isolation. This model, however, is ideally suited to study the implications of events characterized by the simultaneous occurrence of macro and financial shocks spanning multiple horizons, such as financial crises. In this class of nonlinear models, the total effects of, say, two shocks happening simultaneously can be

larger than the sum of their parts.

We look forward to a variety of modifications and extensions of this framework, including but not limited to the following ideas. One could examine the relationships between SV-VAR and DSGE models with time-varying volatility. For instance, DSGE models of stochastic volatility have proven popular in the literature (Justiniano and Primiceri, 2008; Fernández-Villaverde et al., 2015). Moreover, models solved to higher-order approximations generate endogenous volatility through state-dependence. Models with occasionally-binding constraints, along the lines of Guerrieri and Iacoviello (2017), also generate time-varying volatility. A particularly fruitful avenue could be to examine whether these DSGE models generate conditional densities that are in line with those from suitable SV-VARs. A second area of work would be to estimate larger SV-VARs than the one considered in this paper to measure and analyze more sources of uncertainty and risk.

References

Abel, A. B. (1983, March). Optimal Investment under Uncertainty. *American Economic Review 73*(1), 228–233.

Adrian, T., N. Boyarchenko, and D. Giannone (2019). Vulnerable Growth. *American Economic Review 109*(4), 1263–1289.

Adrian, T., F. Grinberg, N. Liang, S. Malik, and J. Yu (2022, July). The term structure of growth-at-risk. *American Economic Journal: Macroeconomics 14*(3), 283–323.

Arias, J. E., J. F. Rubio-Ramírez, and D. F. Waggoner (2018). Inference based on structural vector autoregressions identified with sign and zero restrictions: Theory and applications. *Econometrica 86*(2), 685–720.

Aruoba, S. B., M. Mlikota, F. Schorfheide, and S. Villalvazo (2022). Svars with occasionally-binding constraints. *Journal of Econometrics 231*(2), 477–499. Special Issue: The Econometrics of Macroeconomic and Financial Data.

Baker, S. R., N. Bloom, and S. J. Davis (2016). Measuring Economic Policy Uncertainty. *Quarterly Journal of Economics 131*(10), 1593–1636.

Bar-Ilan, A. and W. C. Strange (1996, June). Investment Lags. *American Economic Review 86*(3), 610–622.

Basu, S. and B. Bundick (2017). Uncertainty Shocks in a Model of Effective Demand. *Econometrica 85*(3), 937–58.

Bekaert, G. and G. Wu (2000). Asymmetric Volatility and Risk in Equity Markets. *Review of Financial Studies 13*(1), 1–42.

Bernanke, B. S. (1983). Irreversibility, Uncertainty, and Cyclical Investment. *Quarterly Journal of Economics 98*(1), 85–106.

Bernanke, B. S., M. Gertler, and S. Gilchrist (1999). The financial accelerator in a quantitative business cycle framework. In J. B. Taylor and M. Woodford (Eds.), *Handbook of Macroeconomics*, Volume 1 of *Handbook of Macroeconomics*, Chapter 21, pp. 1341–1393. Elsevier.

Bloom, N. (2009). The impact of Uncertainty Shocks. *Econometrica 77*, 623–68.

Bocola, L. (2016). The Pass-Through of Sovereign Risk. *Journal of Political Economy 124*(4), 879–926.

Caldara, D., C. Fuentes-Albero, S. Gilchrist, and E. Zakrajšek (2016). The macroeconomic impact of financial and uncertainty shocks. *European Economic Review 88*, 185–207.

Carriero, A., T. Clark, and M. Marcellino (2018). Measuring Uncertainty and Its Impact on the Economy. *Review of Economics and Statistics 100*(5), 799–815.

Carriero, A., T. E. Clark, and M. Marcellino (2023). Capturing Macroeconomic Tail Risks with Bayesian Vector Autoregressions. *Journal of Money, Credit, and Banking*.

Cascaldi-Garcia, D., D. D. Datta, T. R. T. Ferreira, O. V. Grishchenko, M. R. Jahan-Parvar, J. M. Londono, F. Loria, S. Ma, M. del Giudice Rodriguez, and J (2023). What is Certain about Uncertainty? *Journal of Economic Literature*.

Christiano, L. J., R. Motto, and M. Rostagno (2014). Risk Shocks. *American Economic Review 104*(1), 27–65.

Clark, T. E. (2011). Real-Time Density Forecasts From Bayesian Vector Autoregressions With Stochastic Volatility. *Journal of Business & Economic Statistics 29*(3), 327–41.

Cogley, T. and T. J. Sargent (2005). Drift and Volatilities: Monetary Policies and Outcomes in the Post WWII U.S. *Review of Economic Dynamics 8*(2), 262–302.

Creal, D. D. and J. C. Wu (2017). Monetary Policy Uncertainty and Economic Fluctuations. *International Economic Review 58*(4), 1317–54.

Del Negro, M. and F. Schorfheide (2013). DSGE Model-Based Forecasting. In G. Elliott, C. Granger, and A. Timmermann (Eds.), *Handbook of Economic Forecasting*, Volume 2, pp. 57–140. Elsevier.

Delle Monache, D., A. De Polis, and I. Petrella (2021). Modeling and forecasting macroeconomic downside risk. Technical Report 1324, Bank of Italy.

Elenev, V., T. Landvoigt, and S. V. Nieuwerburgh (2021, May). A Macroeconomic Model With Financially Constrained Producers and Intermediaries. *Econometrica 89*(3), 1361–1418.

Evans, C., J. Fisher, F. Gourio, and S. Krane (2015). Risk Management for Monetary Policy Near the Zero Lower Bound. *Brookings Papers on Economic Activity 46*(1), 141–219.

Fernández-Villaverde, J., P. Guerrón-Quintana, K. Kuester, and J. Rubio-Ramírez (2015). Fiscal Volatility Shocks and Economic Activity. *American Economic Review 105*(11), 3352–84.

Gertler, M. (2012). Comment on 'Which Financial Frictions? Parsing the Evidence from the Financial Crisis of 2007 to 2009'. In *NBER Macroeconomics Annual*, Volume 27 of *NBER Chapters*, pp. 215–223. National Bureau of Economic Research, Inc.

Geweke, J. and C. Whiteman (2006). Chapter 1 bayesian forecasting. Volume 1 of *Handbook of Economic Forecasting*, pp. 3–80. Elsevier.

Gilchrist, S., J. W. Sim, and E. Zakrajšek (2014, April). Uncertainty, Financial Frictions, and Investment Dynamics. NBER Working Papers 20038, National Bureau of Economic Research, Inc.

Gilchrist, S. and E. Zakrajšek (2012). Credit Spreads and Business Cycle Fluctuations. *American Economic Review 102*, 1692–1720.

Gorodnichenko, Y. and S. Ng (2017). Level and Volatility Factors in Macroeconomic Data. *Journal of Monetary Economics 91*, 52 – 68.

Guerrieri, L. and M. Iacoviello (2017). Collateral Constraints and Macroeconomic Asymmetries. *Journal of Monetary Economics 90*(C), 28–49.

Hartman, R. (1972, October). The effects of price and cost uncertainty on investment. *Journal of Economic Theory 5*(2), 258–266.

Jacquier, E., N. G. Polson, and P. E. Rossi (2004). Bayesian analysis of stochastic volatility models with fat-tails and correlated errors. *Journal of Econometrics 122*(1), 185–212.

Jermann, U. and V. Quadrini (2012, February). Macroeconomic Effects of Financial Shocks. *American Economic Review 102*(1), 238–271.

Jurado, K., S. Ludvigson, and S. Ng (2015). Measuring Uncertainty. *American Economic Review 105*(3), 1177–1216.

Justiniano, A. and G. E. Primiceri (2008). The Time-Varying Volatility of Macroeconomic Fluctuations. *American Economic Review 98*(3), 604–41.

Koop, G., M. H. Pesaran, and S. M. Potter (1996). Impulse Response Analysis in Nonlinear Multivariate Models. *Journal of Econometrics 74*(1), 119–47.

Ludvigson, S. C., S. Ma, and S. Ng (2021). Uncertainty and business cycles: Exogenous impulse or endogenous response? *American Economic Journal: Macroeconomics 13*(10), 369–410.

Mumtaz, H. (2018). A Generalised Stochastic Volatility in Mean VAR. *Economics Letters 173*(C), 10–14.

Mumtaz, H. and F. Zanetti (2013). The Impact of the Volatility of Monetary Policy Shocks. *Journal of Money, Credit and Banking 45*(4), 535–58.

Oi, W. Y. (1961). The desirability of price instability under perfect competition. *Econometrica 29*(1), 58–64.

Orlik, A. and L. Veldkamp (2014). Understanding Uncertainty Shocks and the Role of Black Swans. Working Paper 20445, National Bureau of Economic Research.

Plagborg-Møller, M., L. Reichlin, G. Ricco, and T. Hasenzagl (2020, Spring). When is growth at risk? *Brookings Papers on Economic Activity 1*, 167–229.

Primiceri, G. E. (2005). Time Varying Structural Vector Autoregressions and Monetary Policy. *Review of Economic Studies 72*(3), 821–52.

Rubio-Ramirez, J. F., D. F. Waggoner, and T. Zha (2010). Structural vector autoregressions: Theory of identification and algorithms for inference. *The Review of Economic Studies 77*(2), 665–696.

Scotti, C. (2016). Surprise and Uncertainty Indexes: Real-Time Aggregation of Real-Activity Macro Surprises. *Journal of Monetary Economics 82*, 1–19.

Shin, M. and M. Zhong (2020). A New Approach to Identifying the Real Effects of Uncertainty Shocks. *Journal of Business & Economic Statistics 38*(2), 367–79.

Van Nieuwerburgh, S. and L. Veldkamp (2006, May). Learning asymmetries in real business cycles. *Journal of Monetary Economics 53*(4), 753–772.

ONLINE APPENDIX
Macroeconomic and Financial Risks:
A Tale of Mean and Volatility

Dario Caldara[*]   Chiara Scotti[†]   Molin Zhong[‡]

April 21, 2023

---

[*]International Finance Division, Federal Reserve Board, Washington DC; dario.caldara@frb.gov.
[†]Federal Reserve Bank of Dallas; chiara.scotti@dal.frb.org.
[‡]Division of Financial Stability, Federal Reserve Board, Washington DC; molin.zhong@frb.gov.

Contents

List of Figures

A   Properties of the Conditional Distribution

In this section, we discuss how different elements of the model presented in equations (1) and (2) relate to the conditional distribution. We focus on the effects of shocks on the mean and volatility of the conditional distribution given one parameterization of the model. Therefore, we abstract away from the effects of estimation uncertainty. Figure A.1 shows the associated conditional distributions.

Conditional Mean Shifts   A homoscedastic version of the model, shown in equation (A.1), can generate movements in the conditional distribution through shifts in the conditional mean:

$$z_t = c + \beta z_{t-1} + \exp\left(\frac{1}{2}\alpha\right) e_t$$
$$e_t \sim N(0,1)$$

(A.1)

The important parameter that governs the strength of this effect is β. If we set $\beta > 0$, the effects on z_t of shocks to e_t linger, which shifts around the conditional mean of the conditional distribution. Therefore, time periods of higher-than-average downside risks follow strings of negative shocks to e_t, when z_t is below its long-run average. The top panel of Figure A.1 shows how the conditional distributions and downside risks change following a negative level shock. The blue line shows the one-step ahead conditional distribution of z_{t+1} when z_t is at its unconditional mean, which is 0. The orange line shows a conditional distribution assuming a lower value for the mean of z_{t+1}. The lower conditional mean of the conditional distribution naturally leads to a higher downside risk.

Assuming a constant volatility, however, implies that the shape of the distribution beyond the conditional mean stays fixed. All one-step ahead density predictions from the model in equation (A.1) are normally distributed with variance of $\exp(\alpha)$. Therefore, the conditional distributions are always symmetric around the conditional mean, with shortfall and longrise (downside and upside risks) moving in lockstep.

Conditional Volatility Shifts   A heteroscedastic version of the model with no feedback between mean and volatility, shown in equation (A.2), can generate movements in the conditional distribution through shifts in the conditional volatility:

$$z_t = c + H_t^{1/2} e_t$$
$$\tilde{h}_t = \alpha + \theta \tilde{h}_{t-1} + S^{1/2} \eta_t$$
$$H_t = \exp\left(\tilde{h}_t\right)$$
$$\begin{pmatrix} e_t \\ \eta_t \end{pmatrix} \sim N\left(\begin{pmatrix} 0 \\ 0 \end{pmatrix}, \begin{pmatrix} 1 & 0 \\ 0 & 1 \end{pmatrix}\right)$$

(A.2)

The volatility of the level shock $\epsilon_t = H_t^{1/2} e_t$ is now stochastic and persistent. To isolate the effects of stochastic volatility alone on the conditional distributions, we shut down any dependence, contempo-

raneous or lagged, between the level and volatility equations. We also remove lags of z_t from the level equation.

Volatility is the key driver of changes to the conditional distribution. The second panel of Figure A.1 shows an example. The blue distribution has a conditional mean of zero and assumes that h_t is at its unconditional mean. The orange line shows the conditional distribution conditional on a large positive volatility shock that realizes at time t. The added volatility raises the left tail risk. This increase in risk is symmetric, however, so the upper tails of the distribution get pushed out simultaneously.[1]

Conditional Mean and Volatility Shifts through Lags Feedback.   We next consider a version of the model that allows for feedback between the level and volatility equation through the lag structure:

$$
\begin{aligned}
z_t &= c + \beta z_{t-1} + H_t^{1/2} e_t \\
\tilde{h}_t &= \alpha + d_1 z_{t-1} \\
H_t &= \exp\left(\tilde{h}_t\right) \\
e_t &\sim N(0,1)
\end{aligned}
\tag{A.3}
$$

The restricted model in equation (A.3) allows for GARCH-type effects, and is closely related to the parametric model estimated in Adrian et al. (2019) and Carriero et al. (2023). Level shocks are allowed to affect volatility with a lag. In this model, a level shock can generate shifts in the conditional mean and volatility of the one-step ahead conditional distribution if $\beta, d_1 \neq 0$. This is because a movement in z_t generates changes in the $t+1$ volatility of e_t and the conditional mean of z_{t+1}.

The bottom panel of Figure A.1 shows in orange the one-step ahead predictions generated by this model with $d_1 < 0$ and following a negative shock to e_t. For comparison purposes, the blue distribution is repeated from the top panel. Following the negative level shock, the mean of the conditional distribution shifts down and the variance increases simultaneously. This shift is such that the downside risk in the variable increases, as evidenced by the leftward move in the 5th percentile relative to the blue distribution. At the same time, however, the upper tail does not change, as the 95th percentiles from the two distributions lie on top of each other. This is because, while the mean of the orange distribution is lower than the blue distribution, its volatility is greater as well. The two effects cancel out at the upper tail of the distribution, leading to no movement in the 95th percentile.

---

[1]The conditional distributions are not normally distributed because of the independent randomness from $t+1$ volatility (η_{t+1}) that multiplies the normally distributed component e_{t+1}.

Figure A.1: Conditional Distributions: Restricted Versions of the Baseline Model
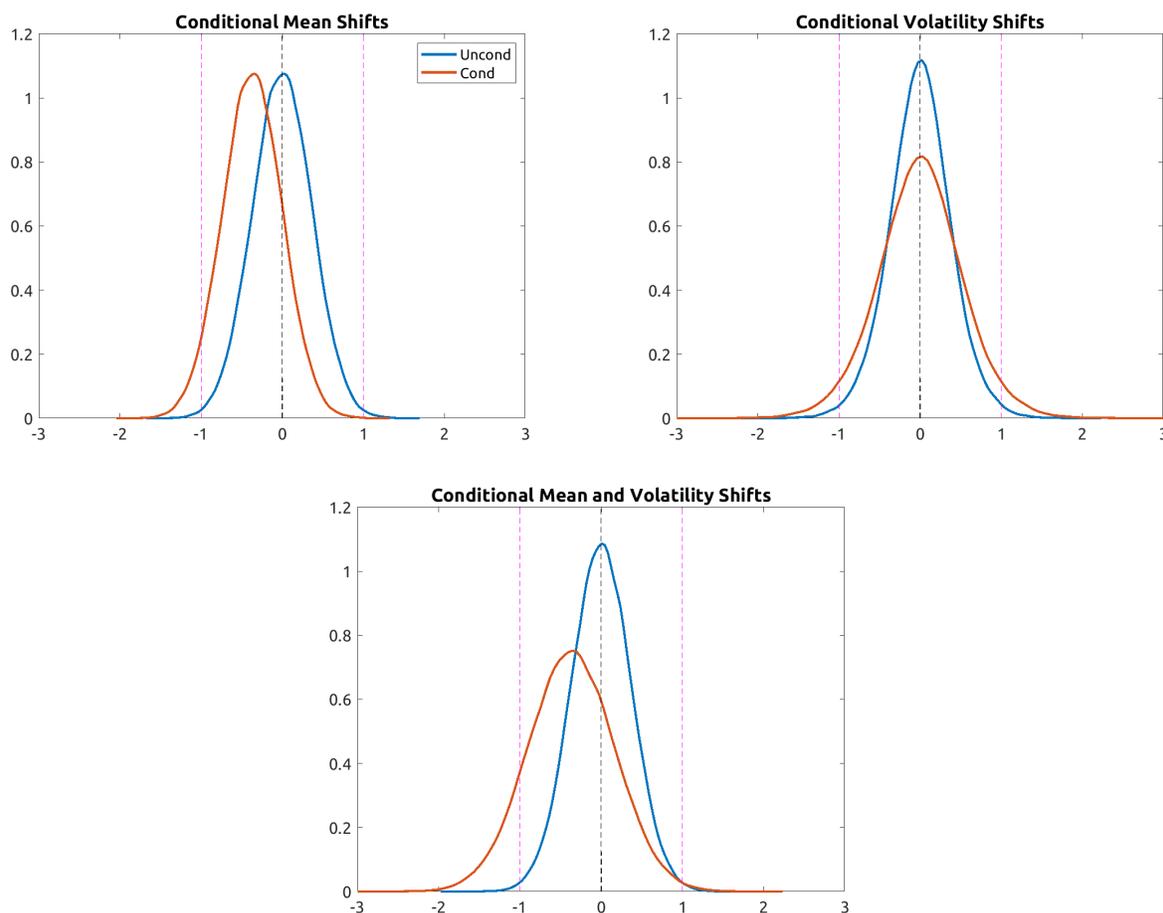
NOTE: This figure plots one-step-ahead conditional densities for three restricted versions of the baseline model. The top left panel shows conditional distributions generated by the model in equation (A.1). The blue line is the unconditional distribution while the orange line is the conditional distribution after a negative 2 standard deviation level shock. The top right panel shows conditional distributions generated by the model in equation (A.2). The blue line is the unconditional distribution with volatility fixed at its mean value while the orange line is the conditional distribution after a positive 2 standard deviation volatility shock. The bottom panel shows conditional distributions generated by the model in equation (A.3). The blue line is a repeat of the blue line in the first panel for comparison purposes, while the orange line shows the conditional distribution after a negative 2 standard deviation level shock. In all cases, the dashed black line shows the mean of the blue distribution while the dashed pink lines show the 5th and 95th percentiles.

B   Discussion about Shock Identification

In this section, we discuss the shock identification. Specifically, we show that Restrictions 1 to 5 are sufficient to identify the four shocks in our model. For convenience, we rewrite the four structural equations of the model reported in the main text:

$$z_{GDP,t} = \underbrace{\eta_{12}}_{<0} z_{CS,t} + \underbrace{\eta_{13}}_{(-1;1)} h_{GDP,t} + \underbrace{\eta_{14}}_{=0} h_{CS,t} + \nu_{M,t}, \tag{A.4}$$

$$z_{CS,t} = \underbrace{\eta_{21}}_{<0} z_{GDP,t} + \underbrace{\eta_{23}}_{(-0.5;0.5)} h_{GDP,t} + \underbrace{\eta_{24}}_{=0} h_{CS,t} + \nu_{F,t}, \tag{A.5}$$

$$h_{GDP,t} = \underbrace{\eta_{31}}_{<0} z_{GDP,t} + \underbrace{\eta_{32}}_{>0} z_{CS,t} + \underbrace{\eta_{34}}_{=0} h_{CS,t} + \nu_{MV,t}, \tag{A.6}$$

$$h_{CS,t} = \eta_{41} z_{GDP,t} + \eta_{42} h_{GDP,t} + \eta_{43} h_{GDP,t} + \nu_{FV,t}. \tag{A.7}$$

The argument of shock identification goes as follows. First, $\nu_{FV,t}$ is uniquely identified by the zero restrictions, as $h_{CS,t}$ only enters in equation (A.7).

Second, $\nu_{MV,t}$ is identified by the sign restriction on η_{31}. To see this, we can rewrite equation (A.6) in terms of structural coefficients:

$$b_{0,33} h_{GDP,t} = b_{0,31} z_{GDP,t} + b_{0,32} z_{CS,t} + b_{0,34} h_{CS,t} + \nu_{MV,t}. \tag{A.8}$$

Note that we normalize the diagonal elements of $B_{0,ss}$ to be positive $b_{0,ii} > 0$. The question we pose is the following: Is it the case that a draw of the structural parameters that satisfy the restrictions imposed in equation (A.6), could also satisfy the restrictions in either equation (A.4) or equation (A.5)? The answer is no. To see this, we can first rearrange equation (A.6) so that GDP growth is on the left hand side and focus only on the elasticity of GDP growth to corporate spreads:

$$z_{GDP,t} = -\frac{b_{0,32}}{b_{0,31}} z_{CS,t}. \tag{A.9}$$

The restrictions on equation (A.6) are such that $b_{0,32} > 0$ and $b_{0,31} < 0$. It follows that $-\frac{b_{0,32}}{b_{0,31}} > 0$, that is, the elasticity of GDP growth to corporate credit spreads is restricted to be positive. Yet, in equation (A.4), we identify $\nu_{M,t}$ by imposing that this elasticity is negative. Hence, a draw of structural parameters that satisfies the sign restrictions to identify $\nu_{MV,t}$ cannot also satisfy the sign restrictions to identify $\nu_{M,t}$. The same argument can be used to show that the structural parameters that satisfy the restrictions imposed in equation (A.6) cannot satisfy the restrictions in equation (A.5).

Third, there is an identification challenge in separating $\nu_{M,t}$ from $\nu_{F,t}$. The restrictions imposed on the elasticities in equations (A.4-A.5) are such that these two shocks are identified for most of the draws, but not all of them. It can be the case that the structural parameters that satisfy the restrictions in equation (A.5) also satisfy the restrictions in equation (A.4). To remove this identification problem, we rely on Restriction 5 and impose that $\nu_{F,t}$ is the shock that explains the most variation in $z_{CS,t}$. It turns out that in our baseline identification, this identification problem does not occur for any draws,

as Restriction 5 is automatically satisfied for all of them.

Figure A.2: Posterior Distribution of Contemporaneous Elasticities
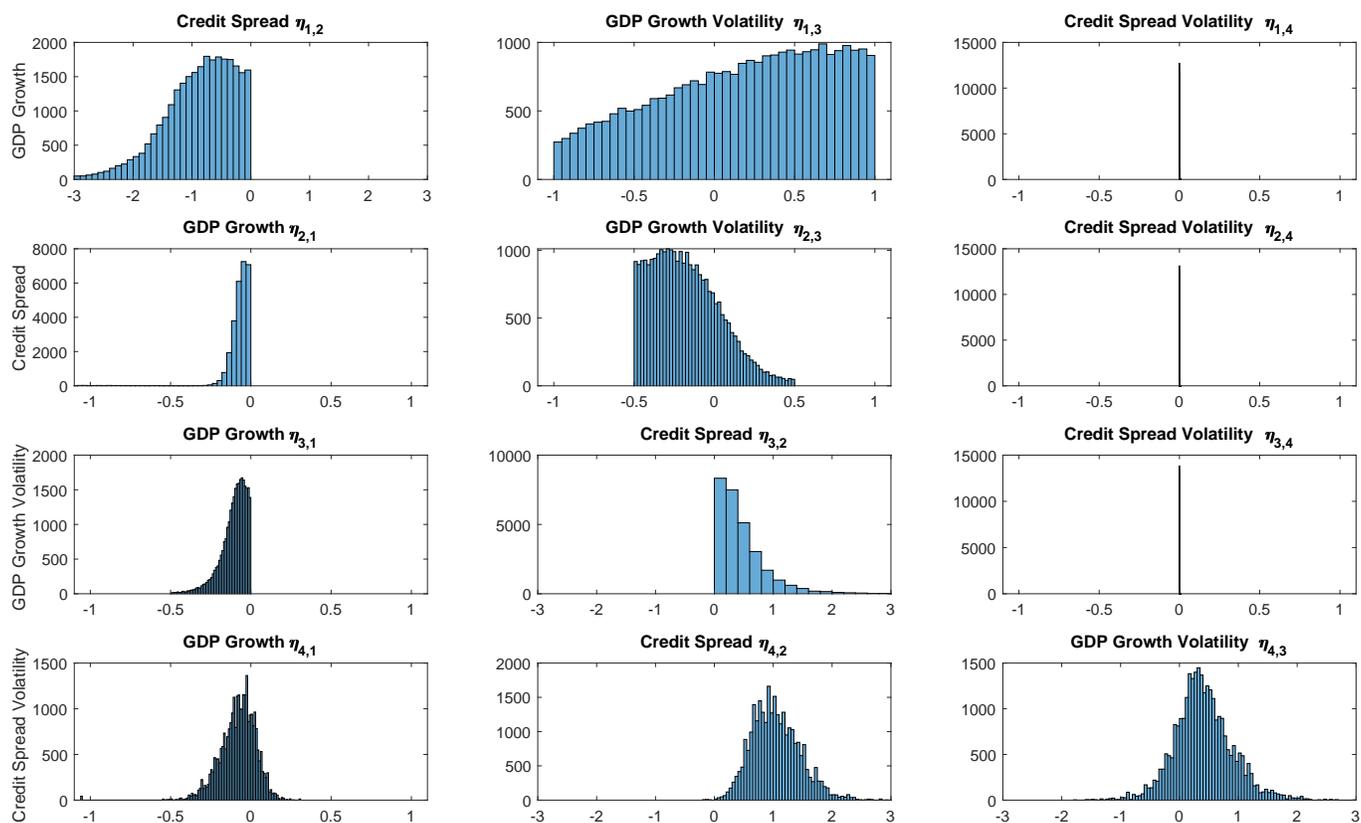
NOTE: The histograms show the posterior distributions of contemporaneous elasticities. The rows correspond to the various equations of the model in structural form, with the first row corresponding to equation (A.4), the second to equation (A.5), the third to equation (A.6), and the fourth to equation (A.7). The titles of each plot indicate the coefficients in each equation.

C Construction of the Conditional Distributions and Impulse Response Functions

We discuss in this section how we construct the baseline and counterfactual posterior conditional distributions to compute our uncertainty and tail risk statistics UIR, SFIR, and LRIR. The conditional distributions are nonstandard objects and we use simulation methods to generate them, following Del Negro and Schorfheide (2013). We also discuss how we construct IRFs.

We begin with how we generate our time T baseline distribution.

Algorithm to Generate Baseline Time T Conditional Distribution

1. For $n = 1, ..., N$:

   Take a parameter draw from the posterior distribution $\{c^n, \beta^n, b^n, \theta^n, d^n, S^n, \Sigma^n, A_0^n, \{h_t^n\}_{t=1}^T\}$.

2. For $m = 1, ..., M$:

   Simulate a path of length F $\{z_{T+1:T+F}^{sim,n,m}, h_{T+1:T+F}^{sim,n,m}\}$ drawing all structural shocks from their assumed distributions. The superscripts contain n to denote that these simulations condition on the nth parameter draw from the posterior distribution.

3. Collect all of the simulations $\{\{z_{T+1:T+F}^{sim,n,m}, h_{T+1:T+F}^{sim,n,m}\}_{m=1}^M\}_{n=1}^N$. We throw out simulations that imply explosive paths. To do so, we discard the paths that imply levels of GDP growth and spreads that are greater than 50 at any point along the path from $T+1$ to $T+F$.[2]

4. Compute posterior statistics of interest, such as uncertainty and tail risk.

We generate our uncertainty and tail risk statistics in Figure 9 by computing these baseline conditional distributions period by period.

Inspired by Gonçalves et al. (2021), we generate counterfactual simulations by *adding* a structural shock of size $\nu_{j,T+1}^* = \delta$ to the baseline simulations. By contrast, Koop et al. (1996) *fix* the structural shock of interest to a value δ, eliminating a source of randomness. Our approach preserves randomness in the period when the shock realizes, which can be of material importance when tracing the effects of the shock on uncertainty and tail risk.[3]

---

[2] In the paper, we focus on the *marginal* posterior conditional distributions. The marginal posterior conditional distribution of variable z_i at forecast horizon f is $p(z_{i,t+f}|\mathcal{I}_t^T) = \int_{z_{-i,t+f}} p(z_{t+f}|\mathcal{I}_t^T) dz_{-i,t+f}$. To calculate the marginal conditional distribution, we integrate the joint density forecast $p(z_{t+f}|z^t)$ over $z_{-i,t+f}$, the forecast at horizon f of all endogenous observed variables except for the variable of interest i. From the marginal densities we can also easily calculate probabilities associated with transformations of z, such as average GDP growth or cumulative growth.

[3] The scope of our paper is different than Gonçalves et al. (2021). They compute impulse responses in linear structural dynamic models that include nonlinearly transformed regressors, by subtracting the counterfactual path from the baseline path simulation by simulation, as they are interested in the mean response. As we are interested in uncertainty and tail risk, we need to first compute them using the counterfactual and baseline densities and then subtract the counterfactual from the baseline. We cannot subtract simulation by simulation to form uncertainty and tail risk responses because these are higher-order moments of the distribution.

Algorithm to Generate Counterfactual Time T Conditional Distribution

1. For $n = 1, ..., N$:

   Take a parameter draw from the posterior distribution $\{c^n, \beta^n, b^n, \theta^n, d^n, S^n, \Sigma^n, A_0^n, \{h_t^n\}_{t=1}^T\}$.

2. For $m = 1, ..., M$:

   Simulate a path of length 1 $\{z_{T+1}^{sim,n,m}, h_{T+1}^{sim,n,m}\}$ drawing all structural shocks from their assumed distributions. The superscripts contain n to denote that these simulations condition on the nth parameter draw from the posterior distribution.

   Add a structural shock j of size $\nu_{j,T+1}^*$ at time $T+1$ to form a counterfactual value $\{z_{T+1}^{*,sim,n,m}, h_{T+1}^{*,sim,n,m}\}$

   Simulate a path of length $F - 1$ starting from the counterfactual values: $\{z_{T+2:T+F}^{*,sim,n,m}, h_{T+2:T+F}^{*,sim,n,m}\}$.

3. Collect all of the simulations $\{\{z_{T+1:T+F}^{*,sim,n,m}, h_{T+1:T+F}^{*,sim,n,m}\}_{m=1}^M\}_{n=1}^N$. We throw out simulations that imply explosive paths. To do so, we discard the paths that imply levels of GDP growth and spreads that are greater than 50 at any point along the path from $T + 1$ to $T + F$.

4. Compute posterior statistics of interest, such as uncertainty and tail risk.

   As we discussed in Section 2, we can form the UIR, SFIR, and LRIR via equations (9)-(10). We now move on to our algorithm to generate IRFs.

Algorithm to Generate Impulse Response Functions Conditional on State at Time T

1. For $n = 1, ..., N$:

   Take a parameter draw from the posterior distribution $\{c^n, \beta^n, b^n, \theta^n, d^n, S^n, \Sigma^n, A_0^n, \{h_t^n\}_{t=1}^T\}$.

2. Compute the conditional expectation for a path of length F $\{E_T\left[z_{T+1:T+F}^n\right], E_T\left[h_{T+1:T+F}^n\right]\}$. The superscripts contain n to denote that these simulations condition on the nth parameter draw from the posterior distribution.

3. At time $T + 1$, consider a 1 unit structural shock of interest $\nu_{T+1}^{j,*} = 1$. We also hold all other structural shocks $\nu_{T+1}^{-j,*} = 0$.

4. Compute a counterfactual conditional expectation of length F

$$\{E_T\left[z_{T+1:T+F}^n | \nu_{T+1}^{j,*} = 1, \nu_{T+1}^{-j,*} = 0\right], E_T\left[h_{T+1:T+F}^n | \nu_{T+1}^{j,*} = 1, \nu_{T+1}^{-j,*} = 0\right]\}.$$

5. To form the IRF, subtract the original path from the counterfactual path as in equation (12).

6. Collect all of the IRF simulations $\{IRF_{F,z}^{j,n}, IRF_{F,h}^{j,n}\}_{n=1}^N$ and compute posterior statistics of interest.

   Note that given the conditional values of z^T, h^T and the shock $\nu_{T+1}^{j,*}$, it is possible to compute the conditional expectations of the system in closed form at any horizon, so we do not have to rely on simulation methods.

D Details on the Estimation Procedure

Our baseline model estimation procedure largely follows Mumtaz (2018), although we implement some modifications suggested by Lindsten et al. (2014) for the particle smoother. Here, we provide the basic steps of the estimation procedure, and refer to Mumtaz (2018) and Lindsten et al. (2014) for details of the posterior sampler. We close the section by presenting some estimation results on simulated data.

Prior distributions Denote $B = \{c_z, c_h, \beta_{1:P}, b_{1:K}, \theta_{1:J}, d_{1:Q}\}$. We use Minnesota-type independent and normally distributed priors for the B parameters. For the parameters in the level equation, we center the constants and first lags at the $AR(1)$ OLS estimates on a presample of data from 1947:Q2 through 1953:Q1. We center the higher-order lags and all cross-lags around 0. For c_z, we set the variance to be $1000^2 \sigma_{i,pre}^2$, where $\sigma_{i,pre}^2$ is the OLS estimates of the innovation variances in the presample. For the lags of the level variables, the variances are of the form $\frac{0.1^2}{l^2}$ for own-lags and $\frac{0.1^2}{l^2} \frac{\sigma_{i,pre}^2}{\sigma_{j,pre}^2}$ for the lag of variable j in equation i. For $b_{1:K}$, we set the prior means to be 0 and the prior variances to be $\sigma_{i,pre}^2$ in equation i.

For the parameters in the volatility equation, we first run an estimation using a VAR model with 4 lags of the observables and exogenous $AR(1)$ stochastic volatility on our entire data sample. We do not assume that there is any relationship between the level and volatility equations in this specification. We then take the posterior mean of the volatility estimates and fit $AR(1)$ models with OLS to them.[4] We center the first lags of the volatility estimates around 0.5. We center the constant and all higher-order lags and cross-lags around 0. We set the variances of the constant to be $\sigma_{i,h}^2$, where $\sigma_{i,h}^2$ is the OLS estimates of the stochastic volatility innovation variances. For the lags of the volatility variables, the variances are of the form $\frac{0.1^2}{l^2}$ for own-lags and $\frac{0.1^2}{l^2} \frac{\sigma_{i,h}^2}{\sigma_{j,h}^2}$ for the lag of variable j in equation i. For $d_{1:Q}$, we set the prior means to be 0 and the prior variances to be $0.1\sigma_{i,h}^2$ in equation i.

We set the priors for the diagonal elements of S as inverse Gamma with 5 degrees of freedom and a mean of 0.04. This is consistent with the literature (Clark, 2011; Carriero et al., 2015).

We put priors on transformed elements of $\Sigma = L^{-1} D L^{-1}$ where L^{-1} is lower triangular and D is diagonal. The priors on elements of L^{-1} are independent $N(0, 1)$ and the prior on elements of D is implicit from the restriction that the diagonal elements of Σ equals 1.

To initialize the stochastic volatility estimation, we assume that h_{-1} is deterministically fixed at the long-run mean implied by the latest draw of the parameters. The time 0 and 1 volatility innovations are assumed to be drawn from independent normal distributions with 0 mean and unit variance. The h_0 value of volatility is then assumed to be its long-run mean plus $S^{1/2} \eta_0$ from the initialization of the volatility innovations.

Posterior Sampler Steps

1. Draw $B|S, \Sigma, h_t$

---

[4]In some cases, the initial volatility estimates are unreasonably large. In that case, we normalize the estimates by dividing by their sample standard deviations and use the normalized series as our initializations.

Conditional upon knowing the sequence of stochastic volatilities, drawing the regression coefficients of the model boils down to a standard problem of linear regression estimation with stochastic volatility. We use the Kalman filter to determine the mean and volatility of the regression parameter draws. After drawing the parameters, we compute the model-implied long-run mean of z_t and h_t. We also simulate the model for 1500 periods to check for explosive dynamics. If the simulated model generates explosive dynamics, we throw out the coefficient draws and draw a new set.

2. Draw $S|B, \Sigma, h_t$

   Drawing S is a nonstandard problem because of the correlation amongst η_t. We use a Metropolis step assuming a mixture of an inverse Gamma distribution using the moments derived from an assumption of independent elements in η_t and a random walk proposal using an inverse Gamma distribution centered on the previous draw. We assume a 20% probability of sampling from the random walk proposal and 80% probability of sampling from the inverse Gamma distribution. For the Metropolis step, we scale the variance of the proposal distribution by 0.01 times the posterior mean of an initial volatility estimate assuming independent AR(1) stochastic volatility processes and no level and volatility interaction.

3. Draw $\Sigma|B, S, h_t$

   We draw Σ using the algorithm of Chan and Jeliazkov (2009). We use a scaling parameter in the Metropolis step of 1.

4. Draw $h_t|B, S, \Sigma$

   We use the particle smoother with ancestor sampling using 80 particles to draw h_t. The further details of the state space form and implementation algorithm can be found in Mumtaz (2018) and references therein. Relative to the algorithm in Mumtaz (2018), we make one modification to the step in calculating the probability of sampling the fixed particle. Mumtaz (2018) calculate this probability only by considering the likelihood of transitioning from the particles in the previous time period to the fixed particle (Step 2.d in the online appendix of the paper). Instead, Lindsten et al. (2014) recommends considering the implications of the fixed particle on the likelihood of the data in the current period and on the future likelihoods. We follow Equation 23 of Lindsten et al. (2014) with $l = 2$.

Estimation of Model on Simulated Data We test our estimation strategy by generating simulated data from a univariate version of baseline model and then using that data to estimate the parameters of the model.

We simulate data from the model with parameters in the bottom row of Table A.1. Our calibration implies that the volatility-in-mean effect, level-in-volatility effect, and correlation between level and volatility innovations are all active. We generate a sample length of $50,000$ from this model and use the both the final 299 and 999 data points to estimate our model.

We use the same prior distributions as in our main estimation strategy. Therefore, we reserve the first 24 data points as a presample. We take $75,000$ draws from the posterior distribution with a burn-in

Table A.1: Results from Estimation on Simulated Data

| Parameter	c_z	β	b_1	c_h	θ	d_1	S	Σ_{12}
90% CS Sample size 275	$[0.82, 1.31]$	$[0.25, 0.46]$	$[-0.32, -0.11]$	$[-0.84, -0.11]$	$[0.48, 0.74]$	$[-0.35, -0.04]$	$[0.10, 0.32]$	$[-0.60, -0.15]$
90% CS Sample size 975	$[0.86, 1.09]$	$[0.41, 0.54]$	$[-0.20, -0.09]$	$[-0.40, -0.01]$	$[0.50, 0.71]$	$[-0.41, -0.16]$	$[0.11, 0.26]$	$[-0.66, -0.40]$
Calibration	1	0.4	-0.2	-0.15	0.7	-0.2	0.2	-0.5

of $50,000$ draws. The posterior sets are computed saving every 25th draw. For the simulation exercise, we use 40 particles in the particle smoother.

The middle two rows in Table A.1 show the results from this exercise. Regardless of whether the sample size is 275 or 975, the 90% posterior credible sets contain the true parameter in all cases but one, which is the β estimate with a sample size of 975. Even in that case, the 90% credible set barely misses and the 95% credible set contains the true value. Moreover, as expected, the credible sets shrink as we increase the sample size.

Figure A.3: IMPULSE RESPONSE FUNCTIONS: VOLATILITY SHOCKS
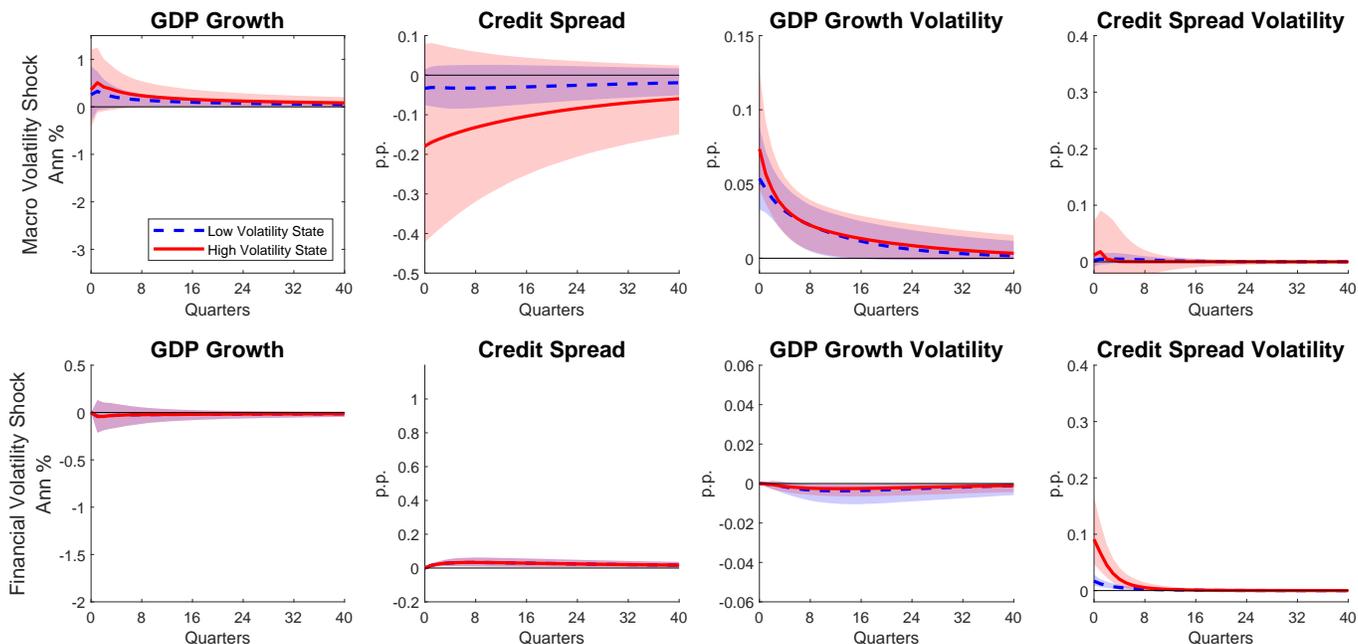
(a) Impulse Response Functions
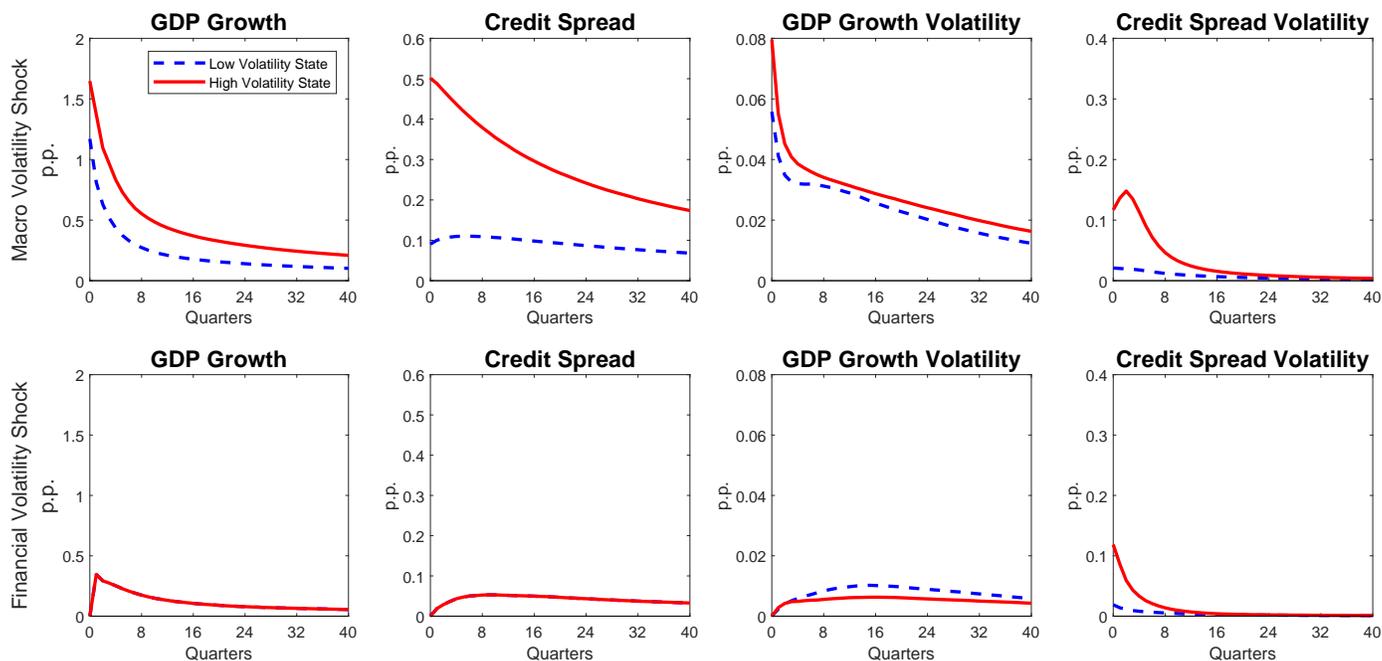
(b) IRFs: Width of Credible Sets

NOTE: The red (blue) lines in the top panel depict the median impulse responses to a one standard deviation macro and financial volatility shock conditioning on 2008:Q4 (2006:Q4), a quarter of high (low) volatility. Shaded areas denote 80 percent credible sets. The volatility responses of the reduced form innovations are in percentage points. The bottom panel depict the width of the 80 percent credible set of the corresponding impulse responses plotted in the top panel. The width of credible sets are all reported in percentage points.

Appendix References

Adrian, T., N. Boyarchenko, and D. Giannone (2019). Vulnerable Growth. *American Economic Review 109*(4), 1263–1289.

Carriero, A., T. E. Clark, and M. Marcellino (2015). Realtime Nowcasting with a Bayesian Mixed Frequency Model with Stochastic Volatility. *Journal of the Royal Statistical Society Series A 178*(4), 837–62.

Carriero, A., T. E. Clark, and M. Marcellino (2023). Capturing Macroeconomic Tail Risks with Bayesian Vector Autoregressions. *Journal of Money, Credit, and Banking*.

Chan, J. C.-C. and I. Jeliazkov (2009). MCMC Estimation of Restricted Covariance Matrices. *Journal of Computational and Graphical Statistics 18*(2), 457–480.

Clark, T. E. (2011). Real-Time Density Forecasts From Bayesian Vector Autoregressions With Stochastic Volatility. *Journal of Business & Economic Statistics 29*(3), 327–41.

Del Negro, M. and F. Schorfheide (2013). DSGE Model-Based Forecasting. In G. Elliott, C. Granger, and A. Timmermann (Eds.), *Handbook of Economic Forecasting*, Volume 2, pp. 57–140. Elsevier.

Gonçalves, S., A. M. Herrera, L. Kilian, and E. Pesavento (2021). Impulse Response Analysis for Structural Dynamic Models with Nonlinear Regressors. *Journal of Econometrics*.

Koop, G., M. H. Pesaran, and S. M. Potter (1996). Impulse Response Analysis in Nonlinear Multivariate Models. *Journal of Econometrics 74*(1), 119–47.

Lindsten, F., M. I. Jordan, and T. B. Schön (2014). Particle gibbs with ancestor sampling. *Journal of Machine Learning Research 15*(63), 2145–2184.

Mumtaz, H. (2018). A Generalised Stochastic Volatility in Mean VAR. *Economics Letters 173*(C), 10–14.